Synthesis, Photochemistry, and Molecular Structures of Peripherally-Molybdenated Tetraphenylporphyrins and -metalloporphyrins

Natalie M. Rowley,* Stefan S. Kurek, Jean-Dominique Foulon, Tom A. Hamor, and Christopher J. Jones

School of Chemistry, University of Birmingham, Edgbaston, Birmingham B15 2TT, U.K.

Jon A. McCleverty*

School of Chemistry, University of Bristol, Cantocks Close, Bristol BS8 1TS, U.K.

Stephan M. Hubig

Department of Chemistry, University of Houston, Houston, Texas 77204-5641

Eric J. L. McInnes, Nicholas N. Payne, and Lesley J. Yellowlees

Department of Chemistry, University of Edinburgh, Edinburgh EH9 3JJ, U.K.

Received January 24, 1995[⊗]

The peripherally-molybdenated tetraphenylporphyrin complexes [5-{*p*-, *m*-, and *o*-[Mo(NO)Tp*Cl]OC_6H_4}-10,15,20-Ph_3porphH_2] (**1**−**3**, respectively; Tp* = [HB(3,5-$Me_2C_3HN_2)_3$], tris(3,5-dimethylpyrazolyl)borate; Ph_3-porphH_2 = triphenylporphyrin) and [5-{*p*-[Mo(NO)Tp*X]OC_6H_4}-10,15,20-Ph_3porphH_2] (X = OH, **4**; X = I, **5**), the metalloporphyrins [5-{*p*-[Mo(NO)Tp*X]OC_6H_4}-10,15,20-Ph_3porphM] (M = Zn, **6**; M = Ni, **7**; M = Pt, **8**), and the tetramolybdenated compound [5,10,15,20-{*p*-[Mo(NO)Tp*Cl]OC_6H_4}$_4$porphH_2] (**9**) have been prepared by reaction of the corresponding 5-(hydroxyphenyl)-10,15,20-triphenylporphyrin or 5,10,15,20-tetraphenylporphyrin derivative. Cyclic voltammetry shows that most of these complexes undergo two oxidation processes (associated with the porphyrin, internally-metalated or otherwise) and three reduction processes (two associated with the porphyrin and one with the molybdenum fragment). The redox potentials of the molybdenum fragment are little influenced by the presence of the macrocyclic ring, and *vice versa*. Preliminary photochemical measurements have been made on **1**−**3**, which were found to undergo photoinduced intramolecular electron transfer, from the excited singlet state of the porphyrin macrocycle to the molybdenum moiety, yielding charge-separated states with lifetimes in the range 120−220 ps. Further studies, using spectroelectrochemistry and EPR spectroscopy, have been made to investigate the nature of the reduced molybdenum species. The molecular structures of **1** and **3** were determined crystallographically, and it was shown that the Mo−O(phenol) distances were relatively short [1.922(5) Å for **1** and 1.855(23) Å for **3**], consistent with $p_\pi \rightarrow d_\pi$ donation, and that in **3** one of the pyrrole rings of the porphyrin closely approaches one of pyrazolyl rings of the tris(3,5-dimethylpyrazolyl)borate ligand. This is consistent with ^{1}H NMR studies. The Mo−porphyrin centroid distances are 10.51 Å in **1** and 6.69 Å in **3**.

Introduction

The control of energy and/or charge distribution within molecules or molecular arrays is of fundamental importance in the development of molecular electronic systems. In particular, attempts to produce simple models of the early steps in photosynthesis have stimulated considerable interest and research activity in charge separation processes.[1] However, despite the many reported examples of intramolecular electron transfer from porphyrin to organic acceptors, such as quinone, methyl viologen, or pyromellitimide,[2] and the abundant number of systems comprising metal sites and porphyrins which have been synthesized,[3,4] examples of electron transfer to externally but covalently-linked transition metal-based redox centers are very rare. Prior to our own involvement in this very specific topic, there were only three examples where photoinduced electron transfer from a porphyrin moiety to one or more peripherally-attached metal acceptor centers was investigated. The first system to be investigated comprised Eu^{3+} cations bound in benzo-crown-ether cavities attached to the four *meso* positions of a zinc porphyrin moiety.[5] This system did indeed facilitate effective intramolecular electron transfer from the excited triplet state of the metalloporphyrin to Eu^{3+}, but the large Eu^{2+} ion so formed was displaced from the crown ether void so that the reverse electron transfer was bimolecular. The second system to be studied consisted of the oxidized form of 5,10,15,20-(4-ferrocenylphenyl)porphyrin (Fc_4tpp).[6] In this

[⊗] Abstract published in *Advance ACS Abstracts*, July 15, 1995.

(1) Kalyanasudaram, K. *Photochemistry of Polypyridine and Porphyrin Complexes*; Academic Press: London, 1992; Chapter 16.
(2) Fox, M. A.; Chanon, M. *Photoinduced Electron Transfer*; Elsevier: Amsterdam, 1988; Part D, Chapter 6.2.
(3) Morgan, B.; Dolphin, D. *Struct. Bonding* **1987**, *64*, 116−203. Hamilton, A. D.; Rubin, H.-D.; Bocarsly, A. B. *J. Am. Chem. Soc.* **1984**, *106*, 7255−7257.
(4) Montanari, F., Casella, L., Eds. *Metalloporphyrin Catalysed Oxidations*; Kluwer Academic Publications: Dordrecht, The Netherlands, 1994; pp 49−86.
(5) Blondeel, G.; Harriman, A.; Porter, G.; Wilowska, A. *J. Chem. Soc., Faraday Trans. 2* **1984**, *80*, 867−876.

0020-1669/95/1334-4414$09.00/0

example, the ferrocenium centers proved ineffective acceptors for an electron from the excited singlet state of the porphyrin moiety, and two explanations were offered as to why electron transfer might be too slow to compete with fluorescence decay: (i) that the reaction might be so exothermic ($\Delta G°$ *ca.* −1.14 eV) that the electron transfer rate would lie in the Marcus inverted region and be so slow as to be unable to compete with other decay mechanisms; (ii) that photoinduced electron transfer to a metal center might be inherently slow. The third example concerned two systems in which electron transfer to a d^{10} metal center occurred.[7] The systems comprised Ag^+ ions bound in each of two [18]-N_2O_4 receptor molecules covalently bound to opposite sides of a porphyrin ring and connected together *via* either a biphenyl strap or a second porphyrin moiety. The partial displacement of Ag^0 from the [18]-N_2O_4 receptor was proposed as a possible explanation as to why charge recombination was found to occur more slowly than the charge separation process. However, it was clear that the Ag^0 atoms could not be completely dislodged from their macrocyclic receptor groups in these examples, since charge recombination was found to occur *via* first-order kinetics.

The parallel and complementary study of the interaction between two adjacent, but not directly bonded, redox centers can, and has, provided additional important information regarding the mechanisms of electron transfer processes. Such information has been obtained, *inter alia*, from binuclear metal complexes in which each metal-containing fragment is redox-active and connected by bridging ligands of varying length and electronic character. Detailed studies of the Creutz−Taube ion and its relatives have contributed very substantially to the understanding of electron-transfer theory,[8] while our investigation of the redox-active binuclear complexes [{Mo(NO)Tp*Cl}$_2$Q] [Tp* = HB(3,5-$Me_2C_3HN_2$)$_3$, tris(3,5-dimethylpyrazolyl)borate; Q = dianionic bridging group] has contributed to the development of a highly flexible system for exploring the dependence on the bridging group Q of electrochemical coupling between the redox centers.[9] A complementary spin-off our work has been the recognition that the coordinatively unsaturated 16-valence-electron {Mo(NO)Tp*}$^{2+}$ group is extremely electronegative, acting as a very powerful polarizing group in dipolar systems[10] and readily undergoing one-electron addition, affording the reduced 17-valence-electron {Mo(NO)Tp*}$^+$ center.[11]

While our initial interest in combining porphyrin species with these molybdenum nitrosyl moieties was driven by an interest in the interactions between a metal-free macrocyclic redox system and a reducible metal nitrosyl group as a contrast to the behavior of two adjacent metal redox centers, we quickly realized that photoexcitation of the porphyrin could lead to the generation of a powerful reducing agent closely attached to a very effective acceptor. Were electron transfer to occur, it would represent a fourth example of photoelectron transfer from a porphyrin ring to an externally attached metal acceptor center in a noncomplementary coordination environment. Furthermore, we knew that the energy of the LUMO in the 16-valence-electron acceptor could be mediated by appropriate adjustment of the metal center (Mo or W) and by substitution of the coligand X (halide, OH, amide, etc.) in the type of compound we believed we could prepare, *viz.* [{Mo(NO)Tp*X}−porphyrin group].

Since we had already established synthetic procedures for making complexes of the general type [M(NO)Tp*Cl(ZC_6H_4)] (M = Mo or W; Z = O or NH) from simple phenols and anilines,[11-13] an extension to appropriately functionalized tetraarylporphyrins was logical and feasible. We have made a preliminary report of our success in attaching peripheral {Mo(NO)Tp*X} groups to tetraphenylporphyrin derivatives and identified photoinduced intramolecular electron transfer from the macrocycle to the metal nitrosyl fragment as a viable and rapid process.[14] Very recently, Enemark and his colleagues reported the attachment of an oxomolybdenum(V) center {MoTp*(O)Cl} to the periphery of a porphyrin ring and described the electrochemical properties of these analogues of our nitrosyl species.[15]

In this paper we describe how we achieved our first objective of attaching the molybdenum nitrosyl acceptor units to a tetraphenylporphyrin ring, via a phenolic linkage. Also described is the full characterization of *para. meta,* and *ortho* isomers of [5-{[Mo(NO)Tp*Cl]OC_6H_4}-10,15,20-Ph_3porphH_2], **1**−**3**, respectively, the tetrametallic complex [5,10,15,20-{*p*-[Mo(NO)Tp*Cl]OC_6H_4}$_4$porphH_2], **9**, as well as derivatives in which the Cl at the molybdenum center is substituted by OH, **4**, and I, **5**, and in which the hydrogen atoms within the porphyrin ring are replaced by Zn^{2+}, **6**, Ni^{2+}, **7**, and Pt^{2+}, **8**. The electrochemical properties of these new complexes and the crystal structures of **1** and **3** have also been determined.

Although these interesting compounds were initially made for solution electrochemical studies, our observation that the compounds were luminescence-quenched prompted a preliminary photochemical study. Thus, our second objective rapidly developed into a study of the effect of varying $\Delta G°$ for photostimulated charge separation on the rates of forward electron transfer from the porphyrin moiety to the {Mo(NO)Tp*X} group by manipulation of the energy of the LUMO, the presumed acceptor orbital, through alternation of the nature of X. We have also used spectroelectrochemical techniques, for example by examination of the electronic and EPR spectra of [**1**]$^-$, to support our view that the LUMO on the molybdenum center is probably the receptor of the phototransferred electron.

We have also investigated the nonlinear optical behavior of this class of compound, and one of the species, **1**, exhibited

(6) Schmidt, E. S.; Calderwood, T. S.; Bruice, T. C. *Inorg. Chem.* **1986**, *25*, 3718−3720.
(7) Gubelmann, M.; Harriman, A.; Lehn, J.-M.; Sessler, J. L. *J. Phys. Chem.* **1990**, *94*, 308−315.
(8) Creutz, C. *Prog. Inorg. Chem.* **1983**, *30*, 1−73. Zhang, L.-T.; Ko, J.; Ondrechan, M. J. *J. Am. Chem. Soc.* **1987**, *109*, 1666−1671. Ondrechan, M. J.; Ko, J.; Zhang, L.-T. *J. Am. Chem. Soc.* **1987**, *109*, 1672−1676. Fürholz, U.; Joss, S.; Bürgi, H.-B.; Ludi, A. *Inorg. Chem.* **1985**, *24*, 943−948. Joss, S.; Bürgi, H.-B.; Ludi, A. *Inorg. Chem.* **1985**, *24*, 949−954. Citrin, P. H.; Ginsberg, A. P. *J. Am. Chem. Soc.* **1981**, *103*, 3673−3679. Fürholz, U.; Bürgi, H.-B.; Wagner, F. E.; Stebler, A.; Ammeter, J. H.; Krausz, E.; Clark, R. J. H.; Stead, M. J.; Ludi, A. *J. Am. Chem. Soc.* **1984**, *106*, 121−123. Stebler, A.; Ammeter, J. H.; Fürholz, U.; Ludi, A. *Inorg. Chem.* **1984**, *23*, 2764−2767.
(9) Charsley, S. M.; Jones, C. J.; McCleverty, J. A.; Neaves, B. D.; Reynolds, S. J.; Denti, G. *J. Chem. Soc., Dalton Trans.* **1988**, 293−299. Charsley, S. M.; Jones, C. J.; McCleverty, J. A.; Neaves, B. D.; Reynolds, S. J. *J. Chem. Soc., Dalton Trans.* **1988**, 301−307. Das, A.; Maher, J. P.; McCleverty, J. A.; Navas Badiola, J. A.; Ward, M. D. *J. Chem. Soc., Dalton Trans.* **1993**, 681−686.
(10) Coe, B. J.; Foulon, J.-D.; Hamor, T. A.; Jones, C. J.; McCleverty, J. A.; Bloor, D.; Cross, G. H.; Axon, T. L. *J. Chem. Soc., Dalton Trans.* **1994**, 3427−3439; **1995**, 673−684.
(11) Cook, R.; Maher, J. P.; McCleverty, J. A.; Ward, M. D.; Wlodarczyk, A. *Polyhedron* **1993**, *12*, 2111−2119.
(12) McCleverty, J. A.; Denti, G.; Reynolds, S. J.; Drane, A. S.; El Murr, N.; Rae, A. E.; Bailey, N. A.; Adams, H.; Smith, J. M. A. *J. Chem. Soc., Dalton Trans.* **1983**, 81−89.
(13) Briggs, T. N.; Jones, C. J.; McCleverty, J. A.; Neaves, B. D.; El Murr, N.; Colquhoun, H. M. *J. Chem. Soc., Dalton Trans.* **1985**, 1249−1254. Al Obaidi, N.; Chaudhury, M.; Clague, D.; Jones, C. J.; Pearson, J. C.; McCleverty, J. A.; Salam, S. S. *J. Chem. Soc., Dalton Trans.* **1987**, 1733−1736.
(14) Rowley, N. M.; Kurek, S. S.; George, M. W.; Hubig, S. M.; Beer, P. D.; Jones, C. J.; Kelly, J. M.; McCleverty, J. A. *J. Chem. Soc., Chem. Commun.* **1992**, 497−499.
(15) Basu, P.; Raitsimring, A. M.; LaBarre, M. J.; Dhawan, I. K.; Weibrecht, J. L.; Enemark, J. H. *J. Am. Chem. Soc.* **1994**, *116*, 7166−7176.

significant secondary harmonic generation as a solid (SHG efficiency 1.93 times that of urea at 1906 nm).[16]

Experimental Section

General Details. All reactions were carried out under an oxygen-free, dry nitrogen atmosphere. Dry, freshly distilled dichloromethane or toluene was used for all reactions. Triethylamine was dried over sodium. The starting materials [Mo(NO)Tp*X_2] (X = Cl or I) were prepared by following known procedures.[17] The *para*, *meta*, and *ortho* isomers of [($MeOC_6H_4$)Ph_3porphH_2] and [(HOC_6H_4)Ph_3porphH_2] and the *para* isomers of [($MeOC_6H_4$)$_4$porphH_2] and [(HOC_6H_4)$_4$porphH_2] were prepared as described in the literature.[18a,19] New compounds were purified by column chromatography (column lengths *ca.* 0.3 m) using Kiesel gel 60 (Merck; 70−230 mesh) or activated alumina UG1 (Phase Sep; 100 mesh). IR spectra were recorded by a PE297 spectrophotometer using KBr disks. ^{1}H NMR spectra were recorded using a JEOL GX-270 (270 MHz) spectrometer and a Bruker AC300 (300 MHz) spectrometer, and NOE spectra were provided by Drs. R. J. Goodfellow and M. Murray of the School of Chemistry, University of Bristol, using a JEOL JNM GX-400 spectrometer. Mass spectra were recorded using a Kratos MS80RF instrument, and fast-atom-bombardment (FAB) spectra were obtained using an 8 kV argon gun, samples being mounted in a NOBA matrix. FAB spectra were also obtained from the SERC Mass Spectrometry Service Centre, University College of Wales, Swansea, again using a NOBA matrix. Absorption spectra were obtained using a Shimadzu UV-240 spectrophotometer.

Singlet-state lifetimes were measured by the single-photon-counting method using a synchronously pumped, cavity dumped Nd-YAG dye laser, as described before.[20] The time resolution of this instrument is *ca.* 100 ps. Data processing was performed with the methods described by O'Connor and Phillips.[21] The reported lifetimes were reproducible to within 0.1 ns.

Flash photolysis experiments were performed with either nanosecond or picosecond time resolution. For the former studies, a frequency-doubled Q-switched Nd-YAG laser was used as excitation source and a pulsed Xe arc lamp was used as monitoring beam. Laser intensities were attenuated by using crossed polarizers. The picosecond studies were achieved with a frequency-doubled mode-locked Nd-YAG laser as excitation source. The 1064 nm fundamental output was used to generate a white light continuum for use as the monitoring beam. The monitoring light was collected with a diode array spectrograph at different delay times. Solutions for flash photolysis were adjusted to have an absorbance of *ca.* 0.1 at 532 nm. Data analysis was made by computer least-squares fitting to appropriate kinetic equations, and quoted lifetimes and rate constants have an expected accuracy of ± 10%.

Cyclic voltammetry was carried out using an EG & G Model 174A polarographic analyzer, with *ca.* 10^{-3} mol dm^{-3} solutions under dry N_2 in dry solvents. A Pt bead working electrode was used, with 0.2 mol dm^{-3} [^{n}Bu$_4$N][BF_4] as supporting electrolyte and a scan rate of 200 mV s^{-1}. Potentials were recorded *vs* a saturated calomel reference electrode, and ferrocene was added as an internal standard. The data obtained were reproducible, the experimental error being ±10 mV. All spectroelectrochemical studies were carried out with an Autolab System containing a PSTAT10 potentiostat, using General Purpose Electrochemical System (GPES) Version 3 software, linked to a Hewlett-Packard 7045A X-Y recorder. Positive feedback ohmic compensation was applied for all cyclic voltammograms recorded. Electrochemical experiments employed a Pt micro-working electrode, a Pt counter electrode, and an Ag/AgCl reference electrode. Cells were thermostated using a Haake Model Q thermostated bath circulator. Coulometric experiments utilized an H-type cell with the Pt basket working electrode fritted from the Pt counter electrode. Inert electrolyte, [^{n}Bu$_4$N][BF_4], was used in 0.5 mol dm^{-3} concentration in CH_2Cl_2. All solutions were purged with Ar for 20 min prior to study. Electrogeneration potentials were 150 mV more positive than E_f for the couple.

The optically transparent electrode cell (OTE) for use in UV/vis/near-IR spectrometers has been described previously.[22] EPR spectra were recorded on an X-band Bruker ER200D-SCR spectrometer.

Microanalyses were performed by the Microanalytical Laboratory, School of Chemistry, University of Birmingham.

Preparation of Complexes 1−3. To a solution of [(HOC_6H_4)Ph_3porphH_2] (0.200 g, 0.32 mmol) and [Mo(NO)Tp*Cl_2] (0.16 g, 0.32 mmol) in dry toluene (65 cm^3) was added NEt_3 (0.32 cm^3), and the mixture was refluxed for 3 h. The solvent was then removed *in vacuo* and the residue chromatographed on silica gel using a mixture of dichloromethane and *n*-hexane (1:1 v/v) as eluant. The main brown fraction was collected, the solvent removed *in vacuo*, and the product obtained as purple crystals by recrystallization from dichloromethane/*n*-hexane. It is essential that the complexes remain in contact with the silica gel for the minimum possible time, as decomposition ensues on prolonged contact.

1. Yield: 0.23 g (68%). ^{1}H NMR (270 MHz, $CDCl_3$); δ 8.94 (4H, A_2B_2, J_{AB} = 4.8 Hz, $\Delta\delta_{AB}$ = 0.1 ppm, pyrrole protons of rings A and B), 8.85 (4H, s, pyrrole protons of rings C and D), 8.28 (2H, d, $J_{pp'}$ = 8.8 Hz, H_p and $H_{p'}$ of $OC_6\mathbf{H}_4$porphH_2), 8.23 (6H, m, *ortho* protons of Ph in Ph_3porphH_2), 7.75 (11H, m, *meta* and *para* protons of Ph in Ph_3porphH_2 and H_q and $H_{q'}$ of $OC_6\mathbf{H}_4$porphH_2); 5.97 (1H, s), 5.96 (1H, s), 5.85 (1H, s) ($Me_2C_3\mathbf{H}N_2$); 2.66 (3H, s), 2.46 (3H, s), 2.44 (3H, s), 2.43 (6H, s), 2.37 (3H, s) (($C\mathbf{H_3}$)$_2C_3HN_2$); −2.71 (2H, s, central N**H** of porphyrin ring). Anal. Calc for $C_{59}H_{51}N_{11}BClMoO_2$: C, 65.1; H, 4.7; N, 14.2. Found: C, 64.9; H, 4.8; N, 13.9. FAB MS: *m/z* 1089 (M^+), 1054 (M^+ − Cl), 631 [(HOC_6H_4)Ph_3porphH_2^+]. IR data (KBr disk): 3325w (ν_{NH}), 2930w, 2860w (ν_{CH}), 2550w (ν_{BH}), 1687sh, 1682s (ν_{NO}), 1542m, ($\nu_{C=C}$), 1445s, 1420s, 1387s, 1371s (ν_{C-Me}) cm^{-1}.

2. Yield: 0.23 g (67%). ^{1}H NMR (270 MHz, $CDCl_3$): δ 8.97 (4H, A_2B_2, J_{AB} = 5.1 Hz, $\Delta\delta_{AB}$ = 0.1 ppm, pyrrole protons of rings A and B), 8.83 (4H, m, pyrrole protons of rings C and D), 8.22 (7H, m, *ortho* protons of Ph in Ph_3porphH_2 and H_q of $OC_6\mathbf{H}_4$porphH_2), 8.03 (1H, s, H_p of $OC_6\mathbf{H}_4$porphH_2), 7.95 (1H, dd, $J \approx$ 8.8 Hz, H_r of $OC_6\mathbf{H}_4$porphH_2), 7.81 (1H, d, $J \approx$ 8.4 Hz, H_s of $OC_6\mathbf{H}_4$porphH_2), 7.76 (9H, m, *meta* and *para* protons of Ph in Ph_3porphH_2); 5.92 (1H, s), 5.85 (1H, s), 5.74 (1H, s), ($Me_2C_3\mathbf{H}N_2$); 2.56 (3H, s), 2.39 (6H, s), 2.37 (3H, s), 2.34 (3H, s), 2.33 (3H, s) (($C\mathbf{H_3}$)$_2C_3HN_2$), −2.78 (2H, s, central N**H** of porphyrin ring). Anal. Calc for $C_{59}H_{51}N_{11}BClMoO_2$: C, 65.1; H, 4.7; N, 14.2. Found: C, 65.0; H, 5.0; N, 13.9. FAB MS: *m/z* 1089 (M^+), 631 [(HOC_6H_4)Ph_3porphH_2^+]. IR data (KBr disk): 3310w (ν_{NH}), 2920w, 2845w (ν_{CH}), 2540w (ν_{BH}), 1682sh, 1670s (ν_{NO}), 1530m, ($\nu_{C=C}$), 1437s, 1410s, 1380s, 1360s (ν_{C-Me}) cm^{-1}.

3. Yield: 0.14 g (39%). ^{1}H NMR (270 MHz, $CDCl_3$): δ 8.83 (4H, A_2B_2, unresolved, pyrrole protons of rings C and D), 8.71 (2H, A_2B_2, J_{AB} = 4.8 Hz, $\Delta\delta_{AB}$ = 0.1 ppm, pyrrole protons $H_{a'}$ and $H_{b'}$), 8.36 (2H, A_2B_2, unresolved, pyrrole protons H_a and H_b), 8.29 (6H, m, *ortho* protons of Ph in Ph_3porphH_2), 8.02 (1H, d, J = 6.6 Hz, H_p of $OC_6\mathbf{H}_4$porphH_2), 7.92 (2H, m, overlapping doublet and doublet of doublets, H_s and H_q/H_r of $OC_6\mathbf{H}_4$porphH_2), 7.77 (9H, m, *meta* and *para* protons of Ph in Ph_3porphH_2), 7.59 (1H, dd, $J \approx$ 7.7 Hz split into doublets; J = 1.0 Hz, H_q/H_r of $OC_6\mathbf{H}_4$porphH_2); 5.53 (1H, s, CH^1), 5.17 (1H, s, CH^2), 1.88 (1H, s, CH^3) ($Me_2C_3\mathbf{H}N_2$); 2.30 (3H, s, Me^1), 2.21 (3H, s, Me^2), 1.85 (3H, s, Me^3), 1.40 (3H, s, Me^4), 0.39 (3H, s, Me^5), 0.23 (3H, s, Me^6) (($C\mathbf{H_3}$)$_2C_3HN_2$); −2.96 (2H, s, central N**H** of porphyrin ring). Anal. Calc for $C_{59}H_{51}N_{11}BClMoO_2$: C, 65.1; H, 4.7; N, 14.2. Found: C, 64.8; H, 5.2; N, 14.5. FAB MS: *m/z* 1089 (M^+), 631 [(HOC_6H_4)Ph_3porphH_2^+]. IR data (KBr disk): 3300w (ν_{NH}), 2920w, 2845w (ν_{CH}), 2530w (ν_{BH}), 1660s (ν_{NO}), 1530m, ($\nu_{C=C}$), 1432s, 1410s, 1378s, 1360s (ν_{C-Me}) cm^{-1}.

(16) Coe, B. J.; Kurek, S. S.; Rowley, N. M.; Foulon, J.-D.; Hamor, T. A.; Harmon, M.E.; Hursthouse, M. B.; Jones, C. J.; McCleverty, J. A.; Bloor, D. *Chemtronics* **1991**, *5*, 23−28

(17) Reynolds, S. J.; Smith, C. F.; Jones, C. J.; McCleverty, J. A. *Inorg. Synth.* **1985**, *23*, 4−9.

(18) (a) Adler, A. D.; Longo, F. R.; Finarelli, J. D.; Goldmacher, J.; Assour, J.; Korsakoff, L. *J. Org. Chem.* **1967**, *32*, 476. Adler, A. D.; Longo, F. R.; Shergalis, W. *J. Am. Chem. Soc.* **1964**, *86*, 3145−3149. (b) Fuhrhop, J.-H.; Smith, K. M. *Laboratory Methods in Porphyrin and Metalloporphyrin Research*; Elsevier: Oxford, U.K., 1976.

(19) Milgrom, L. R. *J. Chem. Soc., Perkin Trans 1* **1983**, 2535−2539.

(20) Brookfield, R. L.; Ellul, H.; Harriman, A.; Porter, G. *J. Chem. Soc., Faraday Trans. 2* **1986**, 82, 219−233.

(21) O'Connor, D. V.; Phillips, D. *Time Correlated Single Photon Counting*; Academic Press: London, 1984.

(22) Macgregor, S. A.; McInnes, E.; Sorbie, R. J.; Yellowlees, L. J. In *Molecular Electrochemistry of Inorganic, Bioinorganic and Organometallic Compounds*; Pombeiro, A. J. L., McCleverty, J. A., Eds.; Kluwer Academic Publishers: Dordrecht, The Netherlands, 1993; pp 503−517.

Preparation of Complex 4. A solution of [(*p*-HOC_6H_4)$Ph_3porphH_2$] (0.090 g, 0.14 mmol) and [Mo(NO)Tp*Cl_2] (0.072 g, 0.15 mmol) in dry toluene (65 cm^3) was treated with NEt_3 (0.14 cm^3) and the mixture was refluxed for 3 h. The solvent was then removed *in vacuo*, and the residue dissolved in dichloromethane, and the solution chromatographed over alumina using chloroform as eluant (it should be noted that the chloro complex decomposes selectively on alumina, giving the hydroxide; this does not occur on silica gel). The main brown fraction was collected, and after evaporation of the solvent *in vacuo*, the complex was obtained as a purple powder after recrystallization from dichloromethane/*n*-hexane. Yield: 0.05 g (31%). ^{1}H NMR (270 MHz, $CDCl_3$): δ 8.93 (4H, A_2B_2, J_{AB} = 4.9 Hz, $\Delta\delta_{AB}$ = 0.1 ppm, pyrrole protons of rings A and B), 8.85 (4H, s, pyrrole protons of rings C and D), 8.25 (8H, m, *ortho* protons of Ph in $Ph_3porphH_2$ and H_p and $H_{p'}$ of $OC_6\mathbf{H}_4porphH_2$), 7.77 (11H, m, *meta* and *para* protons of Ph in $Ph_3porphH_2$ and H_q and $H_{q'}$ of $OC_6\mathbf{H}_4porphH_2$); 6.02 (1H, s), 5.99 (1H, s), 5.87 (1H, s) ($Me_2C_3\mathbf{H}N_2$); 2.67 (3H, s), 2.49 (3H, s), 2.47 (3H, s), 2.46 (6H, s), 2.38 (3H, s) (($C\mathbf{H}_3)_2C_3HN_2$); −2.74 (2H, s, central N**H** of porphyrin ring). Anal. Calc for $C_{59}H_{52}N_{11}BMoO_3$: C, 66.2; H, 4.9; N, 14.4. Found: C, 66.4; H, 5.2; N, 14.1. IR data (KBr disk): 3320w (ν_{NH}), 2930w, 2852w (ν_{CH}), 2550w (ν_{BH}), 1692sh, 1665s (ν_{NO}), 1542m, ($\nu_{C=C}$), 1442s, 1420s, 1382s, 1370s (ν_{C-Me}) cm^{-1}.

Preparation of Complex 5. To a solution of [*p*-(HOC_6H_4)Ph_3-$porphH_2$] (0.050 g, 0.08 mmol) and [Mo(NO)Tp*I_2] (0.05 g, 0.08 mmol) in dry toluene (50 cm^3) was added NEt_3 (0.20 cm^3), and the mixture was refluxed for 3 h. The solvent was then removed *in vacuo* and the residue chromatographed on silica gel using a mixture of dichloromethane and *n*-hexane (1:1 v/v) as eluant. The main brown fraction was collected, the solvent removed *in vacuo*, and the product obtained as purple crystals by recrystallization from dichloromethane/*n*-hexane. Yield: 0.07 g (76%). ^{1}H NMR (300 MHz, $CDCl_3$): δ 8.95 (4H, A_2B_2, J_{AB} = 4.8 Hz, $\Delta\delta_{AB}$ = 0.1 ppm, pyrrole protons of rings A and B), 8.85 (4H, s, pyrrole protons of rings C and D), 8.23 (8H, m, *ortho* protons of Ph in $Ph_3porphH_2$ and H_p and $H_{p'}$ of $OC_6\mathbf{H}_4porphH_2$), 7.85 (2H, d, $J_{qq'}$ = 8.5 Hz, H_q and $H_{q'}$ of $OC_6\mathbf{H}_4porphH_2$), 7.75 (9H, m, *meta* and *para* protons of Ph in $Ph_3porphH_2$), 5.98 (3H, m, $Me_2C_3\mathbf{H}N_2$); 2.65 (3H, s), 2.58 (3H, s), 2.53 (3H, s), 2.48 (3H, s), 2.43 (3H, s), 2.30 (3H, s) (($C\mathbf{H}_3)_2C_3HN_2$); −2.73 (2H, s, central N**H** of porphyrin ring). Anal. Calc for $C_{59}H_{51}N_{11}BIMoO_2$: C, 60.1; H, 4.4; N, 13.1. Found: C, 60.1; H, 5.1; N, 12.1. FAB MS: *m/z* 1181 (M^+), 631 [(HOC_6H_4)$Ph_3porphH_2^+$]. IR data (KBr disk): 3310w (ν_{NH}), 2930w, 2850w (ν_{CH}), 2550w (ν_{BH}), 1690sh, 1680s (ν_{NO}), 1542m, ($\nu_{C=C}$), 1440s, 1418s, 1385s, 1368s (ν_{C-Me}) cm^{-1}.

Preparation of Complex 6. To a solution of [(*p*-HOC_6H_4)Ph_3-$porphZn$] (obtained by reaction of [(*p*-HOC_6H_4)$Ph_3porphH_2$] with zinc acetate[18b]) (0.060 g, 0.09 mmol) and [Mo(NO)Tp*Cl_2] (0.042 g, 0.09 mmol) in dry toluene (50 cm^3) was added NEt_3 (0.30 cm^3), and the mixture was refluxed for 2 d. The solvent was then removed *in vacuo* and the residue chromatographed on silica gel using a mixture of dichloromethane and *n*-hexane (1:1 v/v) as eluant. The main brown fraction was collected, the solvent removed *in vacuo*, and the product obtained as a purple powder by recrystallization from dichloromethane/*n*-hexane. Yield: 0.067 g (65%). ^{1}H NMR (270 MHz, $CDCl_3$): δ 9.04 (4H, A_2B_2, J_{AB} = 4.8 Hz, pyrrole protons of rings A and B), 8.95 (4H, s, pyrrole protons of rings C and D), 8.27 (2H, d, $J_{pp'}$ = 8.8 Hz, H_p and $H_{p'}$ of $OC_6\mathbf{H}_4porphH_2$), 8.23 (6H, m, *ortho* protons of Ph in $Ph_3porphH_2$), 7.76 (9H, m, *meta* and *para* protons of Ph in $Ph_3porphH_2$), 7.72 (2H, d, $J_{qq'}$ = 8.8 Hz, H_q and $H_{q'}$ of $OC_6\mathbf{H}_4porphH_2$); 6.00 (1H, s), 5.98 (1H, s), 5.87 (1H, s) ($Me_2C_3\mathbf{H}N_2$); 2.67 (3H, s), 2.47 (9H, s), 2.45 (3H, s), 2.39 (3H, s) (($C\mathbf{H}_3)_2C_3HN_2$). Anal. Calcd for $C_{59}H_{49}$-$N_{11}BClMoO_2Zn$: C, 61.5; H, 4.3; N, 13.4. Found: C, 61.3; H, 4.6; N, 13.15. FAB MS: *m/z* 1151 (M^+), 694 [(HOC_6H_4)$Ph_3porphZn^+$]. IR data (KBr disk): 2930w, 2852w (ν_{CH}), 2550w (ν_{BH}), 1692sh, 1682s (ν_{NO}), 1542m, ($\nu_{C=C}$), 1442s, 1420s, 1382s, 1370s (ν_{C-Me}) cm^{-1}.

Preparation of Complexes 7 and 8. The related complexes **7** and **8** were obtained by procedures similar to that described for **6**, in yields of *ca.* 60% based on [(HOC_6H_4)$Ph_3porphM$].

7. ^{1}H NMR (270 MHz, $CDCl_3$): δ 8.88 (4H, A_2B_2, J_{AB} = 4.9 Hz, pyrrole protons of rings A and B), 8.74 (4H, s, pyrrole protons of rings C and D), 8.06 (2H, d, $J_{pp'}$ = 8.8 Hz, H_p and $H_{p'}$ of $OC_6\mathbf{H}_4porphH_2$), 8.02 (6H, m, *ortho* protons of Ph in $Ph_3porphH_2$), 7.67 (9H, m, *meta* and *para* protons of Ph in $Ph_3porphH_2$), 7.65 (2H, d, $J_{qq'}$ = 8.4 Hz, H_q and $H_{q'}$ of $OC_6\mathbf{H}_4porphH_2$); 5.97 (1H, s), 5.96 (1H, s), 5.84 (1H, s) ($Me_2C_3\mathbf{H}N_2$); 2.65 (3H, s), 2.45 (3H, s), 2.44 (3H, s), 2.43 (3H, s), 2.41 (3H, s), 2.32 (3H, s) (($C\mathbf{H}_3)_2C_3HN_2$). Anal. Calcd for $C_{59}H_{49}$-$N_{11}BClMoO_2Ni$: C, 61.9; H, 4.3; N, 13.5. Found: C, 61.7; H, 4.6; N, 13.6. IR (KBr disk): 2920w, 2870w (ν_{CH}), 2545w (ν_{BH}), 1684sh, 1688s (ν_{NO}), 1540m ($\nu_{C=C}$), 1448s, 1415s, 1390s, 1365s (ν_{C-Me}) cm^{-1}.

8. ^{1}H NMR (270 MHz, $CDCl_3$): δ 8.84 (4H, A_2B_2, J_{AB} = 5.1 Hz, pyrrole protons of rings A and B), 8.75 (4H, s, pyrrole protons of rings C and D), 8.19 (2H, m, H_p and $H_{p'}$ of $OC_6\mathbf{H}_4porphH_2$), 8.16 (6H, m, *ortho* protons of Ph in $Ph_3porphH_2$), 7.73 (9H, m, *meta* and *para* protons of Ph in $Ph_3porphH_2$), 7.69 (2H, m, H_q and $H_{q'}$ of $OC_6\mathbf{H}_4porphH_2$); 5.99 (1H, s), 5.97 (1H, s), 5.86 (1H, s) ($Me_2C_3\mathbf{H}N_2$); 2.66 (3H, s), 2.47 (3H, s), 2.45 (9H, s), 2.36 (3H, s) (($C\mathbf{H}_3)_2C_3HN_2$). Anal. Calcd for $C_{59}H_{49}N_{11}BClMoO_2Pt$: C, 55.3; H, 3.9; N, 12.0. Found: C, 55.1; H, 4.0; N, 12.3. IR (KBr disk): 2925w, 2863w (ν_{CH}), 2555w (ν_{BH}), 1682s (ν_{NO}), 1545m, ($\nu_{C=C}$), 1452s, 1418s, 1390s, 1370s (ν_{C-Me}) cm^{-1}.

Preparation of Complex 9. To a solution of [(*p*-HOC_6H_4)$_4$-$porphH_2$][18a,19] (0.032 g, 0.05 mmol) and [Mo(NO)Tp*Cl_2] (0.100 g, 0.2 mmol) in chlorobenzene (25 cm^3) was added 4-(dimethylamino)-pyridine (0.025 g), and the mixture was refluxed for 3.5 h. The solution was then filtered and the solvent removed *in vacuo*, the residue being chromatographed on silica gel using first a mixture of dichloromethane and *n*-hexane (1:1 v/v) and then pure dichloromethane as eluant. The main brown fraction was collected, and after removal of the solvent *in vacuo*, the complex was obtained as a purple powder by recrystallization from dichloromethane/*n*-hexane (yield 0.031 g, 24%). ^{1}H NMR (270 MHz, $CDCl_3$): δ 9.02 (8H, s, pyrrole protons), 8.30 (8H, d, $J_{pp'}$ = 8.4 Hz, H_p and $H_{p'}$ of $OC_6\mathbf{H}_4porphH_2$), 7.74 (8H, d, $J_{qq'}$ = 8.8 Hz, H_q and $H_{q'}$ of $OC_6\mathbf{H}_4porphH_2$); 6.02 (4H, s), 5.98 (4H, s), 5.87 (4H, s) ($Me_2C_3\mathbf{H}N_2$); 2.68 (12H, s), 2.48 (12H, s), 2.47 (12H, s), 2.46 (24H, s), 2.41 (12H, s) (($C\mathbf{H}_3)_2C_3HN_2$); −2.59 (2H, s, central N**H** of porphyrin ring). Anal. Calcd for $C_{104}H_{114}B_4Cl_4Mo_4N_{32}O_8$: C, 49.8; H, 4.6; N, 17.9. Found: C, 50.1; H, 4.8; N, 17.6. FAB MS: *m/z* 2508 (M^+). IR data (KBr disk): 3300w,b (ν_{NH}), 2910w, 2845w (ν_{CH}), 2530w (ν_{BH}), 1678s (ν_{NO}), 1525m, ($\nu_{C=C}$), 1435s, 1405s, 1375s, 1358s (ν_{C-Me}) cm^{-1}.

Crystal Structure Determinations. Data were collected using an Enraf-Nonius CAD-4 diffractometer (293 K, Mo Kα X-radiation, graphite-monochromator, λ = 0.710 69 Å). Cell dimensions and intensities were measured by $\omega/2\theta$ scans. Complex neutral-atom scattering factors were employed. The structures were solved by the conventional heavy-atom method, and successive difference Fourier syntheses were used to locate all non-hydrogen atoms, followed by final refinements by full-matrix least-squares procedures. Computations were performed on the University of Birmingham IBM 3090 computer with the SHELXS 86[23] and SHELX 76[24] packages. The molecular diagrams were drawn using PLUTO[25] and ORTEP.[26] Scattering factors with corrections for anomalous dispersion were taken from ref 27. Final atomic coordinates are listed in Tables 1 and 2. The results of mean-plane calculations are in Table 3, and selected bond lengths and angles are in Table 4. Estimated standard deviations are relatively large, particularly for **3**, due to the poor quality of the crystals, resulting in a paucity of data. Full listings of H atom coordinates, bond distances and angles, and anisotropic thermal parameters have been deposited with the Cambridge Crystallographic Data Centre, University Chemical Laboratory, Lensfield Road, Cambridge CB2 1EW, U.K.

Structure Determination of 1. Dark purple crystals of **1** (0.3 × 0.2 × 0.2 mm) were grown from CH_2Cl_2/*n*-hexane. A total of 8764 reflections were scanned in the range $2 < \theta < 25°$, and of these, 4221 unique reflections having $F > 2.5\sigma(F)$ were considered observed and were used for the structure solution and refinement. Three standard reflections measured every 2 h showed no significant variation in intensity.

Crystal Data for 1: $C_{59}H_{51}BClMoN_{11}O_2$, M = 1088.3, triclinic,

(23) Sheldrick, G. M. *Acta. Crystallogr.* **1990**, *A46*, 467−473.
(24) Sheldrick, G. M. SHELX 76, Program for Crystal Structure Determination. University of Cambridge, 1976.
(25) Motherwell, W. D. S.; Clegg, W. PLUTO88, Program for Plotting Crystal and Molecular Structures. Cambridge Structural Database System, Users Manual, 1988. Implemented at Manchester Computing Centre.
(26) Johnson, C. K. ORTEP II; Report ORNL-5138; Oak Ridge National Laboratory: Oak Ridge, TN, 1976. Implemented at Manchester Computing Centre.
(27) *International Tables for X-Ray Crystallography*; Kynoch Press: Birmingham, England, 1974; Vol. 4.

Table 1. Fractional Atomic Coordinates ($\times 10^4$) with Esd's in Parentheses and Equivalent Isotropic Temperature Factors (Å^2 $\times$ 10^3)

	x	y	z	U_{eq}[a]
Mo(1)	−2707(1)	−3797(1)	−1228(1)	42
Cl(1)	−1644(3)	−4036(2)	−2333(2)	82
O(1)	−1599(5)	−2573(5)	−403(3)	51
O(2)	−2179(7)	−5243(6)	−676(6)	89
N(1)	4039(6)	−1080(5)	2289(4)	41
N(2)	2522(7)	−1867(6)	3347(4)	45
N(3)	4444(6)	−1436(6)	4505(4)	45
N(4)	5936(7)	−744(6)	3421(4)	46
N(5)	−3075(7)	−2735(5)	−1690(4)	44
N(6)	−4158(7)	−2877(6)	−1870(4)	53
N(7)	−3958(6)	−3694(5)	−459(4)	45
N(8)	−4854(7)	−3577(5)	−744(4)	52
N(9)	−4191(7)	−4964(6)	−2096(4)	48
N(10)	−5098(7)	−4770(6)	−2208(4)	54
N(11)	−2415(7)	−4668(7)	−875(5)	60
B(1)	−5120(10)	−3724(8)	−1697(6)	53
C(1)	−759(8)	−2407(7)	155(5)	45
C(2)	−123(8)	−2975(8)	−17(6)	52
C(3)	758(9)	−2762(8)	568(6)	57
C(4)	1024(8)	−1982(7)	1363(5)	45
C(5)	375(9)	−1419(7)	1530(5)	52
C(6)	−494(8)	−1610(7)	939(6)	48
C(7)	2004(8)	−1733(7)	1995(5)	44
C(8)	1753(8)	−2058(7)	2682(5)	47
C(9)	657(8)	−2673(8)	2805(6)	57
C(10)	776(8)	−2821(8)	3545(6)	56
C(11)	1933(8)	−2309(8)	3893(6)	52
C(12)	2457(8)	−2248(7)	4651(5)	42
C(13)	1703(9)	−2779(9)	5169(6)	57
C(14)	1807(12)	−3606(11)	5255(9)	100
C(15)	1209(15)	−4065(13)	5769(11)	131
C(16)	467(12)	−3706(13)	6193(8)	101
C(17)	381(12)	−2897(13)	6108(8)	101
C(18)	990(10)	−2427(10)	5606(7)	75
C(19)	3598(8)	−1769(7)	4950(5)	46
C(20)	4119(10)	−1631(8)	5774(5)	62
C(21)	5216(10)	−1261(8)	5803(5)	58
C(22)	5419(8)	−1185(7)	4986(5)	40
C(23)	6457(8)	−915(7)	4745(5)	43
C(24)	7404(8)	−877(8)	5270(5)	51
C(25)	8375(8)	−6(8)	5607(6)	55
C(26)	9248(9)	26(10)	6090(6)	71
C(27)	9184(10)	−848(11)	6222(6)	72
C(28)	8255(11)	−1683(11)	5896(8)	79
C(29)	7354(9)	−1749(8)	5414(6)	63
C(30)	6685(8)	−747(7)	3990(5)	49
C(31)	7726(9)	−553(8)	3687(6)	56
C(32)	7601(9)	−403(9)	2950(6)	64
C(33)	6487(8)	−506(7)	2786(5)	49
C(34)	6000(8)	−413(7)	2089(5)	43
C(35)	6799(7)	−35(8)	1526(6)	50
C(36)	7559(9)	978(8)	1808(6)	67
C(37)	8307(10)	1304(10)	1305(8)	84
C(38)	8337(10)	649(11)	536(7)	77
C(39)	7608(10)	−351(10)	253(7)	77
C(40)	6823(9)	−696(9)	740(6)	72
C(41)	4875(8)	−659(7)	1882(5)	44
C(42)	4415(9)	−542(8)	1159(6)	53
C(43)	3283(9)	−923(7)	1134(5)	54
C(44)	3060(8)	−1262(7)	1849(5)	42
C(45)	−1200(8)	−1474(8)	−1749(6)	63
C(46)	−2453(8)	−1918(7)	−1888(5)	51
C(47)	−3145(9)	−1549(7)	−2177(6)	58
C(48)	−4213(9)	−2142(8)	−2145(5)	54
C(49)	−5283(10)	−2088(9)	−2364(7)	83
C(50)	−3224(9)	−3705(9)	888(6)	71
C(51)	−4045(9)	−3625(7)	339(6)	55
C(52)	−4980(10)	−3437(7)	566(6)	67
C(53)	−5500(9)	−3413(7)	−137(7)	61
C(54)	−6538(11)	−3245(9)	−259(9)	90
C(55)	−3685(11)	−6467(9)	−2652(7)	88
C(56)	−4451(10)	−5951(8)	−2603(6)	64
C(57)	−5538(10)	−6360(8)	−3023(7)	72
C(58)	−5948(10)	−5621(9)	−2784(6)	74
C(59)	−7075(10)	−5668(10)	−3021(8)	97

[a] U_{eq} = 1/3 (trace of the orthogonalized $\mathbf{U}_{ij}$ tensor).

Table 2. Fractional Atomic Coordinates ($\times 10^4$) and Isotropic Temperature Factors (Å^2 $\times$ 10^3) with Esd's in Parentheses

	x	y	z	U_{iso}
Mo(1)	136(1)	1242(2)	0	*a*
Cl(1)	−1068(5)	256(8)	−96(6)	*a*
N(1)	−270(17)	2845(20)	−2283(11)	50(8)
N(2)	785(13)	3930(19)	−1608(10)	33(6)
N(3)	7(15)	5817(18)	−1952(10)	43(7)
N(4)	−1057(13)	4608(18)	−2631(10)	32(6)
N(5)	−574(18)	2543(23)	−354(13)	58(9)
N(6)	−483(12)	3465(16)	−143(8)	27(6)
N(7)	1016(16)	2292(22)	235(11)	49(8)
N(8)	831(17)	3277(23)	342(12)	58(9)
N(9)	−376(15)	1833(20)	748(11)	48(8)
N(10)	−428(17)	2801(21)	832(12)	51(8)
N(11)	582(19)	275(27)	268(13)	73(10)
O(1)	558(12)	1202(20)	−686(9)	60(6)
O(2)	942(6)	−474(22)	482(12)	83(9)
C(1)	1057(8)	682(25)	−1048(13)	38(8)
C(2)	1435(22)	−196(30)	898(16)	65(12)
C(3)	1987(19)	−633(26)	−1235(14)	41(9)
C(4)	2149(24)	−316(31)	−1709(17)	69(12)
C(5)	1738(24)	567(31)	−1835(18)	68(12)
C(6)	1193(17)	1108(23)	−1517(12)	28(8)
C(7)	822(19)	2064(24)	−1731(13)	36(8)
C(8)	1046(19)	2991(26)	−1471(14)	43(9)
C(9)	1640(17)	3130(22)	−1068(12)	28(8)
C(10)	1737(21)	4062(25)	−925(14)	49(10)
C(11)	1195(19)	4611(27)	−1285(14)	47(10)
C(12)	1081(19)	5663(26)	−1305(14)	43(9)
C(13)	1648(21)	6300(34)	−961(16)	66(10)
C(14)	2509(20)	6252(34)	−1016(15)	63(10)
C(15)	3044(27)	6782(31)	−636(18)	81(14)
C(16)	2619(27)	7347(33)	−290(17)	82(13)
C(17)	1832(25)	7420(32)	−233(16)	78(13)
C(18)	1335(23)	6846(28)	−551(16)	66(12)
C(19)	585(19)	6259(30)	−1635(13)	51(9)
C(20)	540(20)	7271(26)	−1664(14)	48(10)
C(21)	−67(24)	7505(30)	−1997(14)	70(11)
C(22)	−417(19)	6577(25)	−2183(14)	47(10)
C(23)	−1072(19)	6466(25)	−2555(13)	47(9)
C(24)	−1452(18)	7455(24)	−2719(13)	37(8)
C(25)	−1959(23)	7886(30)	−2374(17)	68(12)
C(26)	−2330(23)	8858(36)	−2532(17)	77(12)
C(27)	−2109(24)	9265(32)	−3020(17)	68(12)
C(28)	−1655(19)	8792(29)	−3361(14)	48(9)
C(29)	−1305(21)	7783(29)	−3227(15)	56(11)
C(30)	−1373(17)	5595(22)	−2731(12)	24(7)
C(31)	−2058(19)	5486(26)	−3074(14)	46(10)
C(32)	−2189(23)	4447(30)	−3174(16)	69(12)
C(33)	−1541(17)	3947(23)	−2860(12)	35(8)
C(34)	−1450(20)	2871(26)	−2859(14)	50(10)
C(35)	−2117(16)	2383(24)	−3162(13)	32(8)
C(36)	−2808(25)	2163(32)	−2911(19)	81(14)
C(37)	−3502(27)	1714(32)	−3147(18)	82(14)
C(38)	−3412(24)	1478(31)	−3637(17)	76(13)
C(39)	−2621(24)	1451(33)	−3942(18)	82(14)
C(40)	−1981(27)	1939(30)	−3694(18)	78(13)
C(41)	−848(18)	2389(23)	−2613(13)	37(8)
C(42)	−712(19)	1254(28)	−2614(13)	51(9)
C(43)	−77(18)	1029(23)	−2307(12)	46(9)
C(44)	186(23)	1998(26)	−2080(14)	56(10)
C(45)	−1173(24)	1829(30)	−1166(17)	77(13)
C(46)	−1005(24)	2664(32)	−839(17)	68(12)
C(47)	−1115(19)	3641(30)	−877(15)	56(10)
C(48)	−864(21)	4135(26)	−463(15)	53(10)
C(49)	−857(21)	5220(25)	−312(16)	62(11)
C(50)	2334(21)	1376(30)	172(15)	78(13)
C(51)	1830(20)	2248(27)	273(14)	50(10)
C(52)	2154(25)	3202(32)	386(16)	74(13)
C(53)	1566(24)	3862(37)	445(17)	79(12)
C(54)	1494(26)	4928(32)	555(20)	90(14)
C(55)	−671(23)	236(29)	1290(17)	75(13)
C(56)	−630(21)	1290(33)	1196(15)	63(10)
C(57)	−868(21)	2134(29)	1540(15)	63(12)
C(58)	−715(21)	3039(29)	1337(15)	53(10)
C(59)	−795(24)	3991(32)	1533(18)	82(14)
B(1)	−78(24)	3585(34)	411(17)	62(12)

[a] Refined anisotropically.

Table 3. Distances (Å) of Atoms from the N(1)−C(44)−C(7)−C(8)−N(2)−C(11)−C(12)−C(19)−N(3)−C(22)−C(23)− C(30)−N(4)−C(33)−C(34)−C(41) Plane[a]

atom	1	3	atom	1	3
N(1)	−0.05	−0.05	N(3)	−0.09	−0.01
C(44)	−0.10	−0.08	C(22)	−0.13	−0.06
C(7)	+0.01	−0.10	C(23)	+0.04	−0.06
C(8)	+0.11	+0.06	C(30)	+0.15	+0.01
N(2)	−0.01	−0.01	N(4)	−0.00	−0.04
C(11)	+0.15	+0.10	C(33)	+0.12	+0.10
C(12)	+0.06	+0.09	C(23)	+0.00	+0.11
C(19)	−0.16	−0.06	C(41)	−0.11	−0.02

[a] Esd's are *ca.* 0.01 and 0.03 Å for **1** and **3**, respectively.

Table 4. Selected Bond Lengths (Å) and Bond Angles (deg) for **1** and **3**[a]

	1	3
	Distances	
Mo−N(5)	2.206(10)	2.261(30)
Mo−N(7)	2.129(8)	2.091(27)
Mo−N(9)	2.160(6)	2.198(27)
Mo−N(O)	1.775(11)	1.622(36)
N(O)−O	1.171(16)	1.273(37)
Mo−Cl	2.366(3)	2.382(9)
Mo−O	1.922(5)	1.855(23)
O−C(1)	1.332(12)	1.402(36)
	Angles	
N(5)−Mo−N(7)	85.6(3)	87.1(11)
N(5)−Mo−N(9)	85.3(3)	82.3(11)
N(5)−Mo−N(O)	179.0(3)	175.8(13)
N(5)−Mo−Cl	87.5(2)	87.1(8)
N(5)−Mo−O	84.4(3)	81.5(11)
N(7)−Mo−N(9)	79.5(3)	77.7(10)
N(7)−Mo−N(O)	95.0(4)	95.5(13)
N(7)−Mo−Cl	167.2(2)	165.3(8)
N(7)−Mo−O	90.8(2)	91.3(11)
N(9)−Mo−N(O)	94.0(3)	95.8(13)
N(9)−Mo−Cl	89.2(2)	87.9(7)
N(9)−Mo−O	166.3(4)	160.7(12)
Cl−Mo−N(O)	91.8(3)	89.1(11)
Cl−Mo−O	99.2(2)	101.6(8)
O−Mo−N(O)	96.5(3)	101.1(14)
Mo−O−C(1)	132.7(7)	146.3(22)
Mo−N−O	176.0(8)	179.1(29)
	Torsion Angle	
N(O)−Mo−O−C(1)	+10.3	+3.0

[a] Esd's are in parentheses.

space group $P\bar{1}$, $a = 13.08(2)$ Å, $b = 15.18(2)$ Å, $c = 17.01(1)$ Å, $\alpha = 109.48(8)°$, $\beta = 90.85(9)°$, $\gamma = 112.11(9)°$, $V = 2911$ Å^3, $Z = 2$, $D_c = 1.24$ g cm^{-3}, $F(000) = 1124$, μ(Mo Kα) = 0.311 mm^{-1}.

All non-hydrogen atoms were refined with anisotropic thermal parameters. Hydrogen atoms were placed in calculated positions riding on their respective bonded atoms, except for the imino hydrogen atoms, which were located from difference maps and were included in the least-squares refinement. Refinement converged at $R = 0.063$ ($R_w = 0.088$) with a weighting scheme of $w^{-1} = [\sigma^2(F) + 0.0045F^2]$. The final electron density difference synthesis showed no peaks >+1.0 or <−0.5 e Å^{-3}.

Structure Determination of 3. Crystals of **3** were grown from CH_2Cl_2/*n*-hexane as dark purple plates. A total of 4380 reflections were scanned in the range $2 < \theta < 24°$, and of these, 1503 unique reflections having $F > 2.5\sigma(F)$ were considered observed and were used for the structure solution and refinement. Three standard reflections measured every 2 h showed no significant variation in intensity.

Crystal Data for 3: $C_{59}H_{51}BClMoN_{11}O_2$, $M = 1088.3$, orthorhombic, space group $Pna2_1$, $a = 16.430(18)$ Å, $b = 13.244(6)$ Å, $c = 25.055(13)$ Å, $V = 5451$ Å^3, $Z = 4$, $D_c = 1.33$ g cm^{-3}, $F(000) = 2248$, μ(Mo Kα) = 0.333 mm^{-1}.

Anisotropic thermal parameters for the molybdenum and chlorine atoms and isotropic temperature factors for all other atoms were refined. Hydrogen atoms were placed in calculated positions riding on their respective bonded atoms, except for the imino hydrogen atoms, which were neglected. Refinement converged at $R = 0.074$ ($R_w = 0.074$) with a weighting scheme of $w^{-1} = [\sigma^2(F)]$. The final electron density difference synthesis showed no peaks >+0.478 or <−1.426 e Å^{-3}.

Results and Discussion

Synthetic studies. The monofunctionalized porphyrins [(*p*-, *m*-, and *o*-$MeOC_6H_4$)$Ph_3porphH_2$] were prepared by established procedures[18a] and were demethylated using BBr_3[19] to give the phenolic species [$(HOC_6H_4)Ph_3porphH_2$]. Reaction of these phenols with [Mo(NO)Tp*Cl_2] afforded, in the presence of NEt_3, modest yields of the desired *para-*, *meta-*, and *ortho*-substituted complexes **1**−**3**. The iodo complex, **5**, was prepared similarly from [Mo(NO)Tp*I_2]. These compounds were purified by column chromatography on silica gel using mixtures of dichloromethane and *n*-hexane as eluant. It is essential to ensure that these compounds remain in contact with the column for as short a time as possible, since decomposition occurs on prolonged contact with silica gel. When the product obtained from the reaction between [$(p$-$HOC_6H_4)Ph_3porphH_2$] and [Mo(NO)Tp*Cl_2] was chromatographed on alumina using chloroform as the eluant, **4** was obtained in low yield, presumably as a result of partial hydrolysis on the column.

In order to prepare the heterobimetallic species **6**−**8**, it was necessary to preform [5-(p-HOC_6H_4)-10,15,20-$Ph_3porphM$] (M = Zn, Ni or Pt, and to treat this with [Mo(NO)Tp*Cl_2] in the presence of NEt_3. The tetrametallic complex **9** was obtained in low yields by treatment of [$(p$-$HOC_6H_4)_4porphH_2$] with 4 mol equiv of [Mo(NO)Tp*Cl_2] in the presence of 4-(dimethylamino)pyridine.

The extra-ring molybdenated porphyrins are of limited stability, being very sensitive to acid and decomposing slowly in the solid state. Repurification of the materials is essential prior to any extended spectroscopic examination. The majority of the compounds were satisfactorily characterized by elemental analyses (see Experimental) although the data obtained from **5** were high in hydrogen and low in nitrogen. It is conceivable that this compound was contaminated with **1**, since I/Cl exchange in [tris(pyrazolyl)borato]molybdenum nitrosyl species, particularly in chlorinated solvents, has been detected before.[28] However the spectroscopic data obtained from this compound were consistent with its general purity and our formulation.

IR Spectroscopic Studies. The IR spectra of the new complexes exhibited characteristic frequencies associated with the porphyrin rings and the Tp* ligand. In particular, absorptions in the range 2930−3330 cm^{-1} due to ν_{max}(NH) were observed for complexes **1**−**9** and absorptions were observed in the range 2530−2555 cm^{-1} due to ν_{max}(BH) of Tp* and in the range 1660−1692 cm^{-1} due to ν_{max}(NO) associated with the extra-ring {Mo(NO)Tp*} moiety.[11,12]

The NO stretching frequencies fall in the range normal for species of the type [Mo(NO)Tp*X(OAr)].[29] However, ν_{max}(NO) for complexes **1**−**3** decreases in the isomer order *para* > *meta* > *ortho*, suggesting that the $(OC_6H_4)Ph_3porphH_2$ group donates more electron density to the molybdenum center in the **3** than in **2** and **1**, respectively. Whereas ν_{max}(NO) for **1** is identical, within experimental error (±5 cm^{-1}), to that for **5**, that for **4** is *ca.* 17 cm^{-1} lower in frequency, consistent with the π-donor properties of OH versus halogen. Insertion of a metal into the porphyrin ring, giving **6**−**8**, has no significant effect on ν_{max}(NO), but the NO stretching frequency for tetramolybdenated **9** is 4 cm^{-1} lower than that for the monomolybdenated analogue, **1**.

(28) Wlodarczyk, A.; Kurek, S. S.; Moss, M. A. J.; Tolley, M. S.; Batsanov, A. S.; Howard, J. A. K.; McCleverty, J. A. *J. Chem. Soc., Dalton Trans.* **1993**, 2027−2036.
(29) McCleverty, J. A. *Chem. Soc. Rev.* **1983**, *12*, 331−360.

Table 5. Electronic Spectral Data for [5-(RC_6H_4)-10,15,20-$Ph_3porphH_2$] (R = OMe, OH, OMo(NO)Tp*X) and Related Species

compd/R	solvent	B λ^a (ϵ)^b	Q_y(1,0) λ^a (ϵ)^c	Q_y(0,0) λ^a (ϵ)^d	Q_x(1,0) λ^a (ϵ)^d	Q_x(0,0) λ^a (ϵ)^d
[$Ph_4porphH_2$]	CH_2Cl_2	416 (4.5)	513 (1.8)	547 (7.6)	588 (5.3)	644 (4.3)
R = *p*-OMe	CH_2Cl_2	417 (5.0)	514 (1.8)	549 (8.6)	589 (5.4)	645 (4.6)
	DMF	416 (6.5)	513 (1.8)	548 (9.2)	589 (5.3)	645 (4.9)
R = *m*-OMe	CH_2Cl_2	416 (5.0)	513 (1.9)	547 (7.7)	588 (5.5)	644 (4.3)
	DMF	415 (5.0)	513 (1.9)	547 (7.7)	589 (5.4)	644 (4.3)
R = *o*-OMe	CH_2Cl_2	416 (4.6)	512 (1.9)	547 (7.0)	588 (5.9)	643 (3.3)
	DMF	416 (4.4)	512 (1.7)	546 (6.9)	589 (5.0)	645 (3.8)
p-($MeOC_6H_4)_4porphH_2$	CH_2Cl_2	419 (5.0)	516 (1.7)	553 (1.2)^c	592 (5.2)	648 (7.3)
R = *p*-OH	CH_2Cl_2	416 (4.8)	513 (1.7)	549 (7.7)	589 (5.0)	644 (4.2)
	DMF	417 (4.9)	513 (1.8)	549 (9.8)	589 (5.4)	646 (5.2)
R = *m*-OH	CH_2Cl_2	415 (4.5)	513 (1.7)	547 (6.9)	588 (5.1)	643 (3.7)
	DMF	416 (5.0)	513 (1.8)	547 (7.6)	589 (5.2)	645 (4.1)
R = *o*-OH	CH_2Cl_2	416 (4.4)	512 (1.8)	547 (6.5)	587 (5.5)	643 (3.3)
	DMF	416 (4.7)	513 (1.8)	546 (7.4)	589 (5.2)	645 (3.9)
1	CH_2Cl_2	416 (3.5)	514 (2.2)	550 (9.8)	588 (8.0)	648 (5.1)
	DMF	416 (4.1)	512 (2.3)	549 (1.2)^c	588 (8.7)	647 (5.8)
2	CH_2Cl_2	416 (4.0)	513 (2.2)	547 (1.0)^c	588 (6.3)	643 (4.0)
	DMF	416 (3.6)	513 (2.1)	547 (9.8)	589 (5.6)	645 (3.9)
3	CH_2Cl_2	419 (3.3)	515 (1.8)	549 (7.9)	591 (5.1)	648 (3.0)
	DMF	418 (2.8)	515 (1.6)	548 (7.0)	591 (4.5)	648 (2.9)
5	CH_2Cl_2	416 (4.3)	513 (2.3)	549 (1.0)^c	589 (8.1)	648 (4.7)
	DMF	417 (3.4)	514 (1.8)	551 (1.1)^c	590 (6.4)	647 (5.4)
9	CH_2Cl_2	418 (1.4)	510 (3.3)	555 (1.4)^c	583 (1.2)^c	659 (5.3)
[$Ph_4porphZn$]	CH_2Cl_2	417 (6.6)	546 (2.4)^e		583 (4.0)^f	
	DMF	423 (6.9)	558 (2.2)^e		597 (9.5)^f	
6	CH_2Cl_2	418 (5.0)	547 (2.3)^e		589 (5.9)^f	
	DMF	424 (4.5)	558 (2.0)^e		599 (8.2)^f	

^{a} In nm. ^{b} ϵ in mol^{-1} L cm^{-1} × 10^5. ^{c} ϵ in mol^{-1}L cm^{-1} × 10^4. ^{d} ϵ in mol^{-1} L cm^{-1} × 10^3. ^{e} Q (1,0). ^{f} Q (0,0).

Electronic Absorption Spectra. In dichloromethane and in dimethylformamide solutions all of the compounds show absorption spectra characteristic of the porphyrin group (Table 5). As expected, the compounds containing unmetalated porphyrins show five major absorptions: the intense B or Soret bands at *ca.* 420 nm, and four Q bands in the range 500−650 nm which decrease in intensity with increasing wavelength. In each of the spectra, there is a shoulder at *ca.* 395 nm, which is probably due to the B(1,0) band, *i.e.* containing one quantum of vibrational excitation relative to the Soret band. In addition, there are weak N and L bands between *ca.* 225 and 375 nm. These spectra are largely unperturbed by the position of the OMe or OH groups. However, the absorption bands of [(*p*-$MeOC_6H_4)_4porphH_2$] are shifted bathochromically with respect to those of [(*p*-$MeOC_6H_4)Ph_3porphH_2$], presumably as a result of more extensive electronic interaction between the porphyrin macrocycle and its peripheral groups in the former relative to the latter.

Extra-ring metalation of the porphyrins generally results in a decrease in the intensity of the Soret band and increases in the intensities of the Q bands (Figure 1). However, the molybdenum fragments {Mo(NO)Tp*X(OC_6H_4)} also absorb in the UV/visible region. The spectrum of [Mo(NO)Tp*Cl(OPh)] contains very broad bands (due almost certainly to the overlap of several peaks, as seen in the circular dichroism spectra of [Mo(NO)Tp*Cl(OR)][28]), one extending from *ca.* 380 nm to above 600 nm (λ_{max} = 465 nm; $\epsilon = 6.0 \times 10^3$ mol^{-1} dm^3 cm^{-1}). However, the extinction coefficients of the molybdenum species are generally less than those of the porphyrin fragment in the same region. The absorption at 314 nm in the electronic spectrum of [Mo(NO)Tp*Cl(OPh)] may be due to a $\pi \rightarrow \pi^*$ transition associated with the pyrazolyl rings in Tp*, and the bands at 421 and 465 nm to NO → Mo and Tp* → Mo charge transfer bands.[30] Since the molybdenum moiety absorptions are very weak and broad and overlap with the weak porphyrin bands, it was not felt that they could be accurately studied, so they have been omitted from Table 5 and from the subsequent discussion.

A comparison of the values of λ_{max} in dichloromethane for **1** and **2** and their unmetalated precursors, [($ROC_6H_4)Ph_3porphH_2$] (R = H, Me), shows that the absorptions in the latter are relatively unperturbed on attachment of {Mo(NO)Tp*Cl}. However, the spectra of the *ortho* isomers in dichloromethane reveal that all of the bands move bathochromically by an average of 3 nm on metalation. These shifts are small, the maximum value being 5 nm which corresponds to an energy difference of *ca.* 1.4 kJ mol^{-1}, or *ca.* 15 mV in electronic potential terms.

Tetrametalation of [(*p*-$HOC_6H_4)_4porphH_2$] has a pronounced effect on the electronic spectrum of the porphyrin. For complex **9** in dichloromethane, the Soret band and two of the Q bands undergo hypsochromic shifts of 1−9 nm and the two remaining Q bands undergo bathochromic shifts of 2−11 nm relative to [(*p*-$MeOC_6H_4)_4porphH_2$]. These shifts imply that those absorptions which do not contain a quantum of vibrational excitation are at lower energies than they are in their unmetalated counterparts, whereas those bands containing a quantum of vibrational excitation are at higher energies as a result of the presence of the molybdenum nitrosyl centers. As observed for the monometalated species, the Soret band for the tetrametalated species has a lower intensity than that for [(*p*-$MeOC_6H_4)_4$-$porphH_2$], whereas the ϵ values of the Q bands are generally higher than those for [(*p*-$MeOC_6H_4)_4porphH_2$].

The electronic spectra of [$Ph_4porphZn$] and **6** in dichloromethane exhibit the characteristic Soret band and two Q bands, although the spectrum of the (tetraphenylporphinato)zinc compound reveals two additional weak bands in the Q-region, at 483 and 509 nm, detected by other workers,[31] whereas the monomolybdenated species shows only one additional weak band at 500 nm. The attachment of the molybdenum nitrosyl fragment to [$Ph_4porphZn$] causes a slight bathochromic shift (6 nm) of the Q(0,0) band of **6** and, as expected, a reduction in intensity of the Soret band.

(30) McWhinnie, S. L. W. Personal communication.

(31) Darwent, J. R.; Douglas, P.; Harriman, A.; Porter: G.; Richoux, M.-C. *Coord. Chem. Rev.* **1982**, *44*, 83−126.

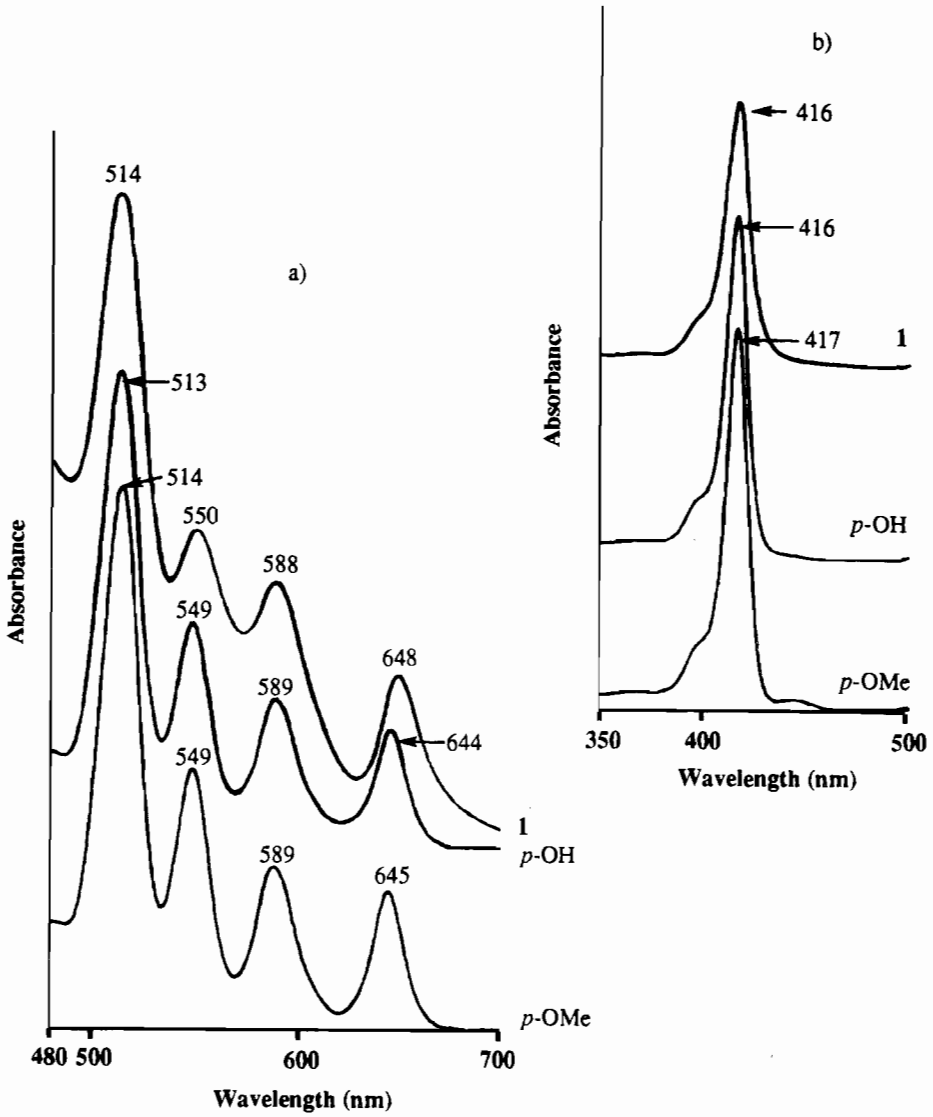

Figure 1. Electronic absorption spectra in CH_2Cl_2 for [5-(*p*-RC_6H_4)-10,15,20-Ph_3porphH_2] (R = OMe, OH, OMo(NO)TP*Cl) at (a) 10^{-5} M showing the Q bands and (b) 10^{-6} M showing the B (Soret) band.

In general, there are few differences between the electronic spectra of these complexes when measured in dichloromethane and in DMF. However, some differences are detected between the spectra of [Ph_4porphZn] and **6**, the complexes having a red-purple color in the former solvent and a blue-purple color in the latter. These effects are almost certainly due to binding of DMF to the Zn center as is known to occur with pyridines.[32]

Spectroelectrochemical UV/vis studies were made on reduced complex **1** to determine how the absorption spectrum between 200 and 400 nm changes upon electrochemical reduction of the molybdenum group. These findings could then be used to help to interpret the findings from the PS UV studies. Prior to reduction, complex **1** in CH_2Cl_2 at 0 °C had very broad, weak absorption bands at *ca.* 230 (this was not studied further, as it was partially obscured by the solvent absorption), 307, *ca.* 348, and *ca.* 365 nm. Upon reduction at −0.7 V, at 0 °C, the original absorption at 307 nm had moved to *ca.* 312 nm and those which had previously occurred at 348 and 365 nm were too broad to be resolved. These studies show that the MoTp* group (and porphyrin moiety) absorbs weakly below 400 nm, thus explaining why no absorption due to the reduced MoTp* moiety could be observed by PS UV studies (see below).

^{1}H NMR Spectra. The 270 MHz ^{1}H NMR spectra of the peripherally metalated porphyrin complexes all contain signals consistent with the presence of the porphyrin ring system and the {Mo(NO)Tp*} moiety (Figure 2). The central N−H protons of the porphyrin ring appear in the range −2.59 to −2.96 ppm.

The signals due to the pyrrolyl protons generally appear in the region $\delta = 8.42-9.04$ ppm, and those for the monometalated species consist of an A_2B_2 system (rings A and B) and a singlet (rings C and D). The A_2B_2 resonances arise because of the presence of the {Mo(NO)Tp*Cl} moiety and appear at a field lower than the other pyrrolyl protons because of the proximity to the electron-withdrawing molybdenum nitrosyl group. The fact that the protons of rings C and D appear as a singlet reveals that there is no coupling between the phenyl and porphyrin rings.[33] The pyrrolyl protons in **9** are equivalent, appearing as a singlet at lower field than the ring A and ring B protons in **1**.

In all of the peripherally monomolybdenated compounds, the *ortho* protons of the unsubstituted porphyrin phenyl rings give rise to an unresolved multiplet at $\delta = 8.02-8.29$ ppm, whereas the *meta* and *para* protons produce an unresolved multiplet at $\delta = 7.67-7.77$ ppm. That the *ortho* protons resonate at fields lower than their *meta* and *para* counterparts could be explained in terms of their proximity to the ring current of the porphyrin ring.

(32) Mashiko, T.; Dolphin, D. In *Comprehensive Coordination Chemistry*; Wilkinson, G., Gillard, R. D., McCleverty, J. A., Eds.; Pergamon Press: Oxford, U.K., 1987; Vol. 2., Chapter 21.1.1, p 814−898. Hunter, C. A.; Sanders, J. K. M.; Beddard, G. S.; Evans, S. *J. Chem. Soc., Chem. Commun.* **1989**, 1765−1767.

(33) Walker, F. A.; Balke, V. L.; McDermott, G. A. *Inorg. Chem.* **1982**, *21*, 3342−3348.

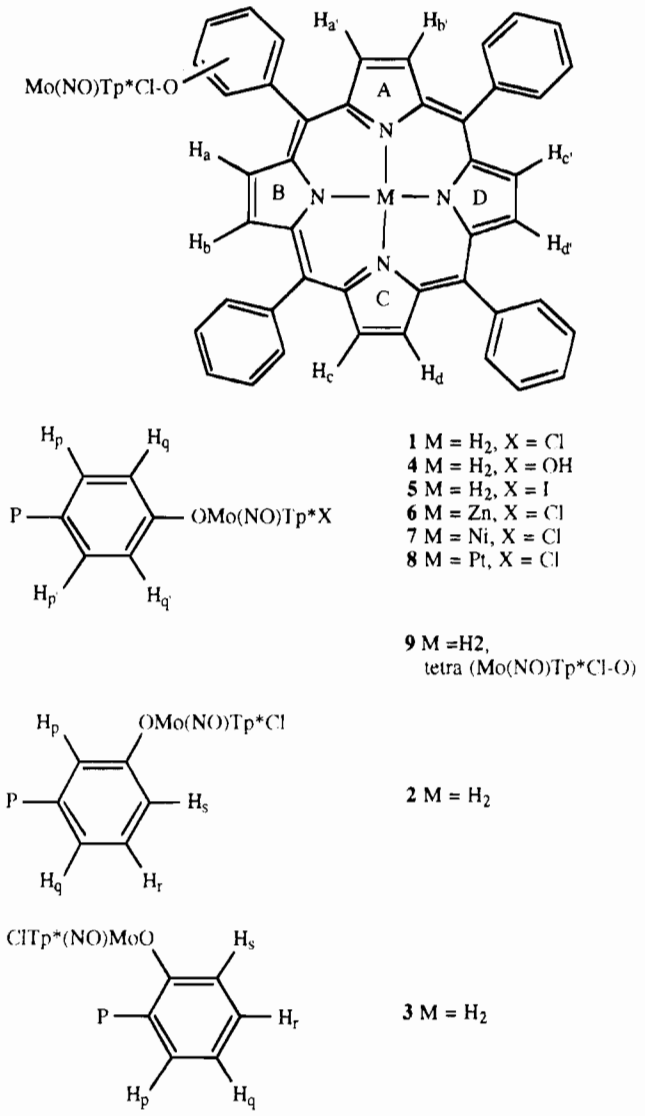

Figure 2. Atom labeling in extra-ring molybdenated porphyrin complexes.

The protons in the molybdenated phenyl ring appear in the range $\delta = 7.59-8.30$ ppm. In some spectra, parts of the signals appear within unresolved multiplets due to the protons of the unsubstituted phenyl rings. In **1** and **4**–**9** the protons H_p, $H_{p'}$ and H_q, $H_{q'}$ (for atom labeling see Figure 2) give rise to two doublets ($^3J_{HH}$ = *ca.* 9 Hz), the former occurring at lower field because it is *ortho* to the electron-withdrawing {Mo(NO)Tp*Cl} group.

The signals of the metalated phenyl ring of **2** appear, from low to high field, as a doublet (H_q), a singlet (H_p), a doublet of doublets (appearing as a triplet) (H_r), and a doublet (H_s), respectively.

The comparable region for **3** gives rise to a doublet (H_p), a doublet and a doublet of doublets (appearing as a triplet) (H_s and H_q/H_r), and a doublet of doublets (H_q/H_r), respectively. The signal due to H_p usually occurs at a field lower than the signals due to H_q, H_r, and H_s, since it is *ortho* to the porphyrin ring.

The unique pyrazolyl 4-protons in Tp* in the porphyrin derivatives usually appear as three singlets, in the range $\delta = 5.74-6.02$ ppm, because of the lack of a symmetry plane in the {Mo(NO)Tp*Cl(OC_6H_4)} group. The methyl protons of Tp* may appear as five or six resonances, in the region $\delta = 2.33-2.68$ ppm, also because of the lack of a plane of symmetry in the group.

A notable exception to these generalizations concerns the ^{1}H NMR spectrum of **3**. It was noted that the pyrrolyl protons give rise to three multiplets, an unresolved A_2B_2 set (H_c $H_{c'}$, H_d, and $H_{d'}$), an AB pair, and an unresolved AB pair ($H_{a'}$ and $H_{b'}$, H_a and H_b). The multiplet at lowest field was assigned to H_c, $H_{c'}$, H_d, and $H_{d'}$ since the overall integral of this resonance was 4 and since the signals due to these protons in other related compounds appear at an identical δ value, although as a singlet. The signals due to H_a $H_{a'}$, H_b, and $H_{b'}$ appear upfield with respect to those of the equivalent protons in the other peripherally-metalated compounds reported here. Another unusual feature is the upfield shift (*ca.* 0.2 ppm) of the NH protons of the porphyrin. Further, while all of the pyrazolyl ring protons of Tp* appear at δ values upfield of those in the *meta*- and *para*-substituted compounds, one pyrazolyl ring proton exhibits a much larger upfield shift than the other Tp* protons, appearing at $\delta = 1.88$ ppm rather than at *ca.* 5.9 ppm.

These observations suggest that there may be close approach of two of the pyrazolyl rings in Tp* to part of the porphyrin ring because of the steric arrangements of the *ortho*-substituted {Mo(NO)Tp*Cl(OC_6H_4}} moiety. In order to investigate this possibility, nuclear Overhauser effect (NOE) studies were made of **3**. Each of the methyl groups in Tp* were individually irradiated, and the increases in the intensity of other peaks were determined (Figure 3): the positions and labeling of the H and methyl protons are shown in Table 6. From these results, the protons in the pyrazolyl rings could be assigned as follows: ring 1—Me^1, Me^3, CH^1; ring 2— Me^2, Me^4, CH^2; ring 3—Me^5, Me^6, CH^3. It was also apparent that irradiation of Me^2 and Me^4 resulted in an enhancement of the signals due to ring 3, and *vice versa*.

Irradiation of Me^2, Me^4, Me^5, and Me^6 all resulted in an enhancement of the signals due to the pyrrolyl protons H_a and H_b. These results suggest that the face of ring B in the porphyrin lies between pyrazole rings 2 and 3 in Tp*.

Electrochemical Studies. The electrochemical properties of the new complexes were examined by cyclic voltammetry in dry dichloromethane using a Pt bead working electrode and [^{n}Bu$_4$N][BF_4] as supporting electrolyte (Table 7).

The unmetalated porphyrins exhibited two reduction and two oxidation processes in the range +1.50 V to −2.00 V (SCE), consistent with one-electron transfer reactions (by analogy with known electrochemical behavior of porphyrin and metallo-porphyrin compounds and by coulometric investigation of **1**). Extra-ring metalation by one {Mo(NO)Tp*(X)} group barely perturbed the E_f values for the porphyrin oxidation processes. However, reduction of the molybdenum center occurred *before* electron transfer to the porphyrin ring, and the E_f values for the first and second reduction potentials of the porphyrin ring in **1** and **2** were *ca.* 50 and *ca.* 100 mV, respectively, more cathodic than those for the analogous unmetalated porphyrins. However, for **3**, both the first and second macrocycle ring reduction potentials are 140 mV more cathodic than those for the unmetalated species. This may be so because of the closer proximity of the {Mo(NO)Tp*Cl} group to the porphyrin in this species than in its *para* and *meta* analogues. The reduction potentials of the {Mo(NO)Tp*Cl} group in **1** and **2** were barely altered by the position of its attachment to the porphyrin ring, although the E_f-value was 50 mV more cathodic for its reduction in **3** than in **1** or **2**, due perhaps to the proximity of the metal center to the porphyrin ring.

The electrochemical behavior of **9** is significantly different from that of the simple unmetalated porphyrins. Thus an

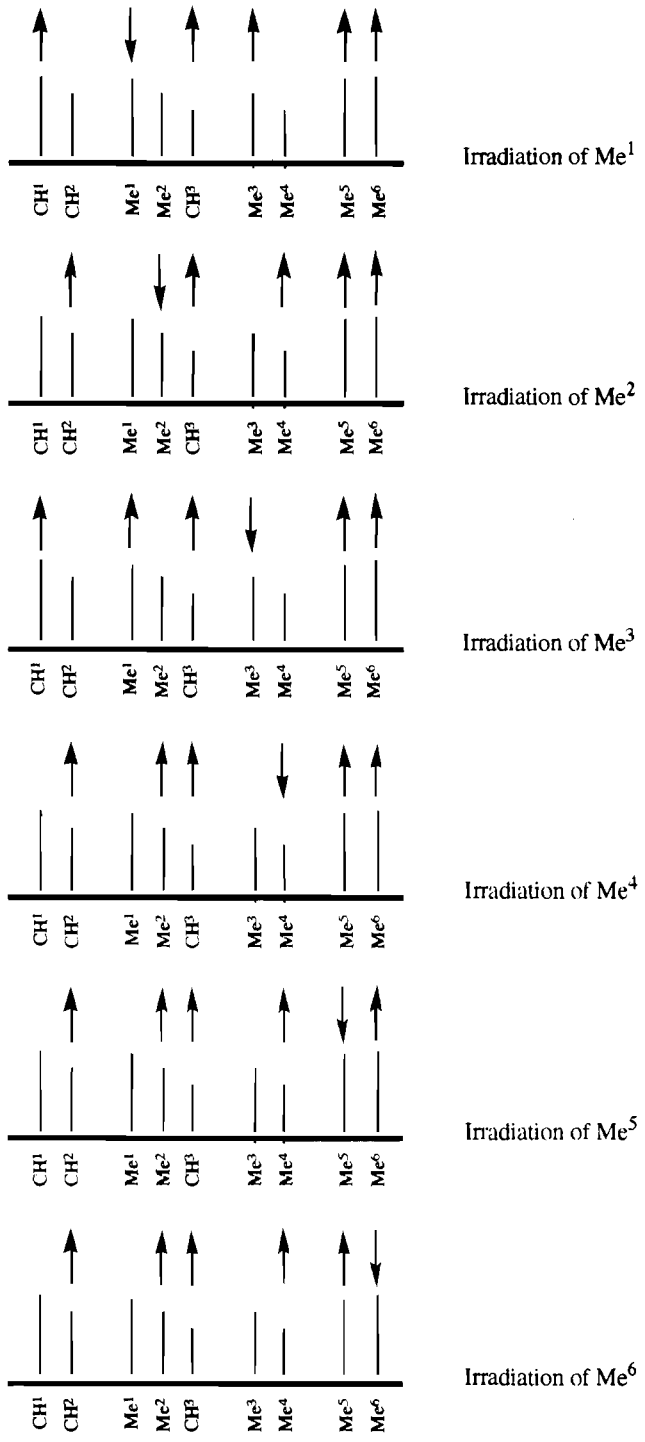

Figure 3. NOE studies of **3**.

irreversible oxidation process at +1.00 V and an irreversible ring reduction at −1.35 V were observed. The cathodic shift of the reduction wave is approximately 4 times the cathodic shift found for the first ring reduction process in **1**. The reduction of the four {Mo(NO)Tp*Cl} groups occurred at effectively the same potential, this being a four-electron reduction. In addition, the reduction wave was very broad, due to the four nearly identical reductions occurring very close together. This suggests that the four {Mo(NO)Tp*Cl} groups are effectively noninteracting.

By varying the nature of X in [5-{*p*-[Mo(NO)Tp*X]OC_6H_4}-10,15,20-Ph_3porphH_2], only the E_f value for the reduction of the Mo center was altered, in the order E_f = I < Cl < OH. This reflects the increasing π-donor properties of the groups X. Finally, it was observed that in the species [5-{*p*-[Mo(NO)-Tp*Cl]OC_6H_4}-10,15,20-Ph_3porphM] (M = Zn, Ni, Pt), the

Table 6. Proton Labeling Used in NOE Investigations of **3**

label	δ/ppm	assignment
CH^1	5.53	pyrazolyl ring protons, $Me_2C_3\mathbf{H}N$
CH^2	5.17	
CH^3	1.88	
Me^1	2.30	pyrazolyl methyl protons, $(\mathbf{CH_3})_2C_3HN_2$
Me^2	2.21	
Me^3	1.85	
Me^4	1.40	
Me^5	0.39	
Me^6	0.23	

oxidation and reduction potentials of the porphyrin ring system were noticeably perturbed, but there was no significant effect on the value of E_f for the reduction of the Mo center.

These data provide additional evidence that there is little ground-state interaction between the porphyrin ring and the {Mo(NO)Tp*Cl} group.

EPR Spectral Studies. The electrochemically reduced 17-electron form of **1** has characteristic signals at room temperature at $g_{iso} = 1.977 \pm 0.001$, with a hyperfine coupling constant of 4.9 ± 0.05 mT and all of the components expected from the different Mo isotopes in their natural abundance.[48] At 77 K, the 17-electron form of **1** gives an axial spectrum (Figure 4) with $g_{\|} = 1.923 \pm 0.001$ and $g_{\perp} = 2.004 \pm 0.001$ and with $A_{\|} = 8.13 \pm 0.05$ mT and $A_{\perp} = 3.76 \pm 0.05$ mT. $(2A_{\perp} + A_{\|})/3 \approx A_{iso}$, and therefore $A_{\perp}$, $A_{\|}$, and A_{iso} all have the *same* sign. $g_{iso} \approx g_{av} = (2g_{\perp} + g_{\|})/3$. There was no obvious coupling with other nuclei.

Photochemical Studies. Preliminary picosecond spectroscopic studies have been carried out on **1**−**3**.[14] Time-correlated single-photon-counting studies of dimethylformamide solutions of **1**−**3** indicate that the fluorescence lifetimes of the molybdenated porphyrins are <15 ps, compared to *ca.* 12 ns measured for nonmolybdenated models ([(*p*-$MeOC_6H_4$)Ph_3porphH_2]), although there is evidence of a very minor long-lived (*i.e.* 10 ns) component which is ascribed to a trace (nonmolybdenated) impurity. Picosecond time-resolved absorption spectroscopy showed that the transient species is nonluminescent and cannot be attributed to a short-lived singlet state. The characteristic absorption at 740 nm in the spectrum provides evidence for the rapid ($k > 3 \times 10^{10}$ s^{-1}; $\tau < 30$ ps) formation of the porphyrin radical cation, which decayed following first-order kinetics with rates in the range $(4.6-8.5) \times 10^9$ s^{-1}, corresponding to lifetimes in the range 120−220 ps (Table 8). From spectroelectrochemical UV/vis studies (see above) it is known that the reduced form of the MoTp* moiety absorbs below 400 nm; thus unfortunately it was not possible to observe its formation and decay by this technique, as it was only possible to monitor the spectrum between 400 and 800 nm. However, the rates of the charge separation and charge recombination are consistent with *intra*molecular processes, and electrochemical techniques show that the Mo moiety is the easiest site to reduce. In addition, spectroelectrochemical EPR studies showed that the one-electron reduction of complex **1** affords a complex containing the 17-electron molybdenum center, so that it may be assumed that the molybdenum atom acts as the acceptor in these complexes.

It has been found that very fast charge separation occurs over a distance of *ca.* 1 nm in these peripherally metalated porphyrins, but charge recombination is relatively slow. A number of reasons may be proposed to account for this difference in rates. The most significant of these regards the ΔG° values for charge separation and charge recombination (Table 8). It is possible that the ΔG° values for charge recombination lie in the Marcus-inverted region (Table 8); *i.e.*, the rate constants decrease with increasing exothermicity ($-\Delta G^\circ$) of the electron-transfer process. The differences in the

Table 7. Electrochemical Data Obtained from [5-(RC_6H_4)-10,15,20-Ph_3porphH$_2$] (R = OMe), [{Mo(NO)Tp*X(OC_6H_4)}Ph_3porphH$_2$], and Related Complexes

	porphyrin				
	oxidn		redn		Mo redn[a]
compd	$E_f(1)^b$ (ΔE_p)[c]	$E_f(2)^b$ (ΔE_p)[c]	$E_f(3)^b$ (ΔE_p)[c]	$E_f(4)^b$ (ΔE_p)[c]	$E_f(5)^b$ (ΔE_p)[c]
R = *p*-OMe	+1.06 (100)[d]	+1.28 (70)[d]	−1.08 (70)[d]	−1.44 (85)[d]	
R = *m*-OMe	+1.09 (65)[e]	+1.35 (55)[e]	−1.09 (65)[e]	−1.44 (55)[e]	
R = *o*-OMe	+1.09 (130)[f]	+1.37 (120)[f]	−1.12 (90)[f]	−1.48 (110)[f]	
1	+1.07 (85)[d]	+1.31 (90)[d]	−1.14 (75)[d]	−1.53 (120)[d]	−0.31 (70)[d]
2	+1.09 (80)[d]	+1.35 (80)[d]	−1.14 (75)[d]	−1.54 (110)[d]	−0.32 (90)[d]
3	+1.07 (75)[f]	+1.35 (80)[f]	−1.26 (80)[f]	−1.62 (135)[f]	−0.36 (85)[f]
4	+1.02 (70)[f]	+1.31 (80)[f]	−1.13 (75)[f]	−1.52 (80)[f]	−0.81 (75)[f]
5	+1.07 (90)[f]	+1.31 (100)[f]	−1.14 (70)[f]	−1.51 (80)[f]	−0.24 (90)[f]
6	+0.91 (40)[f]	+1.17 (60)[f]	−1.29 (45)[f]	−1.68 (70)[f]	−0.32 (45)[f]
7	+1.12 (100)[f]	+1.34 (120)[f]	−1.24 (90)[f]	−1.88[f,g]	−0.32 (120)[f]
8	+1.20 (70)[f]		−1.22 (50)[f]		−0.28 (60)[f]
9	+1.00 (120)[f]		−1.35 (120)[f]		−0.30 (110)[f]

[a] Reduction of {Mo(NO)Tp*X}, in dry CH_2Cl_2 *vs* SCE using Pt bead working electrode; scan rate 200 mV s^{-1}; 0.2 mol dm^{-3} [^{n}Bu$_4$N][BF_4]. [b] In V mol dm^{-3} (±0.01 V). [c] In mV (±10 mV). [d] E_f for couple [Fe(C_5H_5)$_2$]/[Fe(C_5H_5)$_2$]$^+$ = +0.54 V (ΔE_p = 75 mV). [e] E_f for couple [Fe(C_5H_5)$_2$]/[Fe(C_5H_5)$_2$]$^+$ = +0.53 V (ΔE_p = 80 mV). [f] E_f for couple [Fe(C_5H_5)$_2$]/[Fe(C_5H_5)$_2$]$^+$ = +0.55 V (ΔE_p = 80 mV). [g] From differential pulse voltammetry.

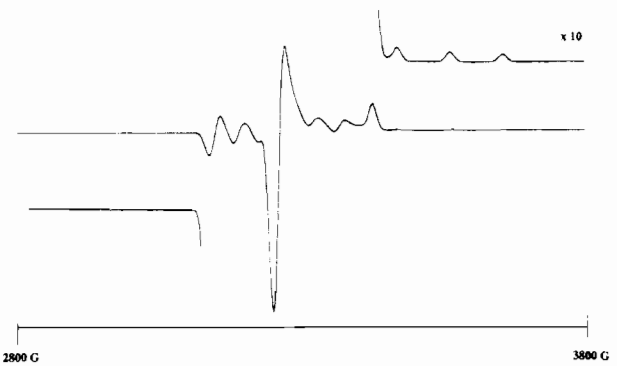

Figure 4. EPR spectrum of the electrochemically reduced 17-electron form of **1** at 77 K.

Table 8. Redox Potentials and Transient Lifetimes

compd	E_f(Mo)/ V[a]	E_f(porph)/ V[a]	k_{CR}/ 10^9 s^{-1}	τ/ps[d]	ΔG^{o}/eV CS[e]	ΔG^{o}/eV CR[e]
1	−0.31	1.07	4.6 ± 0.2[b]	220 ± 7	−0.50	−1.38
2	−0.32	1.09	4.6 ± 0.9[b]	220 ± 4	−0.47	−1.41
3	−0.36	1.07	8.5 ± 0.6[c]	120 ± 9	−0.45	−1.43

[a] *Vs* standard calomel electrode (SCE), measured in dichloromethane containing 0.2 mol dm^{-3} [^{n}Bu$_4$N][BF_4] at a Pt bead electrode. Fc/Fc$^+$ = +0.54 (±0.01) V; E_f(Mo) is the first reduction potential associated with the {Mo(NO)} moiety, and E_f(Porph) is the first oxidation potential associated with the porphyrin moiety. [b] Rate of charge recombination, measured at *ca.* 740 nm. [c] Rate of charge recombination, measured at *ca.* 440 nm. [d] Lifetime of the charge-separated state, based upon k_{CR}. [e] CS = charge separation; CR = charge recombination. Calculated as $\Delta G^{\circ}(CS) = E_f^1 - E_f^2 - E_{singlet} + w^*$ and $\Delta G^{\circ}(CR) = E_f^2 - E_f^1 - w^*$, where E_f^1 and E_f^2 are the measured half-wave potentials for oxidation of the porphyrin and reduction of the {Mo(NO)} moiety, respectively, $E_{singlet}$ is the energy of the first excited singlet state of the porphyrin, and w^* is the Coulombic work term, which here was ignored.

rates may also reflect processes such as slow solvent reorganization.[34] A further possibility is that structural changes associated with the oxidation of the peripheral redox center may be rate-limiting in these systems. Regarding this last possibility, it is notable that the precursor molecules contain 16-electron molybdenum centers in which an sp^2 O donor atom allows mesomeric contact between the molybdenum center and the aryl ring of the tetraphenylporphyrin moiety.[12,29,35] In the charge-separated species, it would be expected that a 17-electron molybdenum center bound to an sp^3 donor atom would be present due to rehybridization of the oxygen and a reduction in the O−Mo p_π−d_π interaction.[36] This would lead to a different geometric arrangement which could affect electron transfer rates.

Structural Studies. Tetraphenylporphyrin itself occurs in two crystalline forms: tetragonal and triclinic. In the tetragonal form[37] the macrocycle is markedly nonplanar, while in the triclinic form[38] the porphyrin shows only small deviations from planarity. Because of crystallographic symmetry in the tetragonal form,[37] the imino hydrogen atoms are equally distributed, with a statistical population of only half a hydrogen atom on each nitrogen atom. This is attributed to a statistical distribution between two orientations rotated 90° around the 4-fold inversion axis. In the triclinic form,[38] the hydrogen atoms are localized on one pair of nitrogen atoms. In order to assess the structural effects on the porphyrin of peripheral metalation and obtain an accurate value of the Mo−porphyrin distance, the molecular structures of **1** and **3** were determined crystallographically. These structures are shown in Figures 5 and 6, final atomic coordinates in Tables 1 and 2, results of mean-plane calculations in Table 3, and selected bond distances and angles in Table 4.

The porphyrin central NH hydrogen atoms of **3** could not be found on the difference Fourier map and so were not included. However, in **1**, the hydrogen atoms were located on a pair of facing nitrogen atoms.

The bond lengths and bond angles obtained for the porphyrin moieties in **1** and **3** are in agreement with those obtained for tetraphenylporphyrin, within the rather large experimental errors.[37,38]

The porphyrin skeleton in the tetragonal form of tetraphenylporphyrin is ruffled;[37] *i.e.*, there is a deformation of the porphyrin skeleton below the plane of the ring, as defined by the inner ring atoms, in the first and third quadrants and above the plane of the porphyrin ring in the second and fourth. Maximum deviations, alternately above and below the ring plane, occur at the methine carbon atoms with the nitrogen atoms close to the plane. Mean plane calculations show that in **1** and **3** the porphyrin inner rings are not planar, but ruffled, with atomic deviations up to 0.16 and 0.11 Å, respectively (Table 3). The porphyrin ring in **1** ruffles in a regular manner, with

(34) Harrison, R. J.; Pearce, B.; Beddard, G. S.; Cowan, J. A.; Sanders, J. K. M. *Chem. Phys.* **1987**, *116*, 429−448.
(35) McWhinnie, S. L. W.; Jones, C. J.; McCleverty, J. A.; Hamor, T. A.; Foulon, J.-D. *Polyhedron*, **1993**, *12*, 37−43.
(36) Al Obaidi, N.; Hamor, T. A.; Jones, C. J.; McCleverty, J. A.; Paxton, K.; Howes, A. J.; Hursthouse, M. B. *Polyhedron* **1988**, *7*, 1931−1938.
(37) Hamor, M. J.; Hamor, T. A.; Hoard, J. L. *J. Am. Chem. Soc.* **1964**, *86*, 1938−1942. Hoard, J. L.; Hamor, M. J.; Hamor, T. A. *Ibid.* **1963**, *85*, 2334−2335.
(38) Silvers, S. J.; Tulinsky, A. *J. Am. Chem. Soc.* **1967**, *89*, 3331−3337.

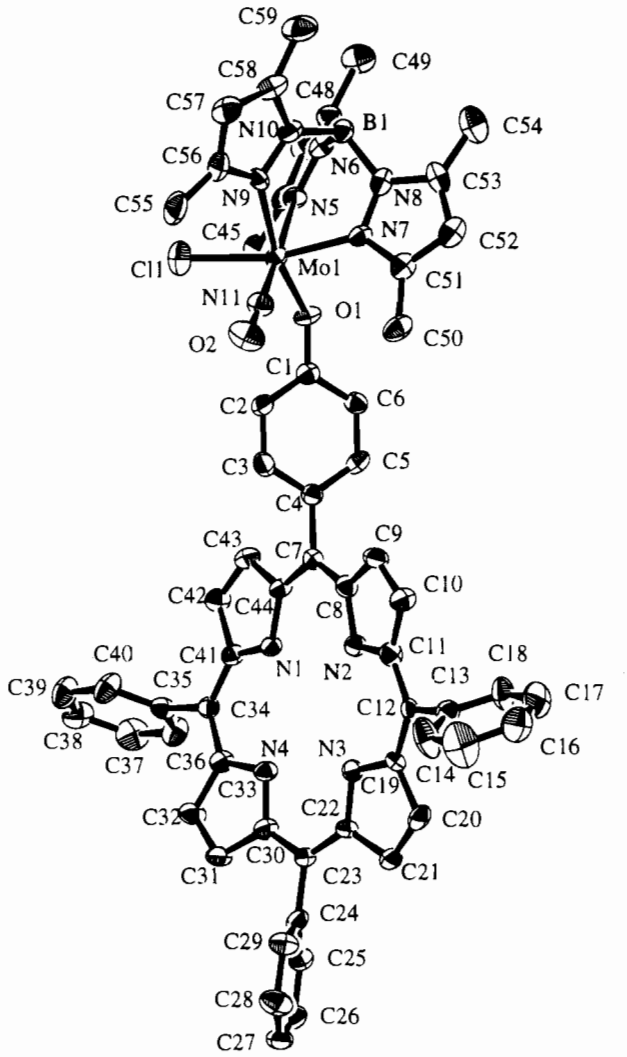

Figure 5. Molecular structure of **1**.

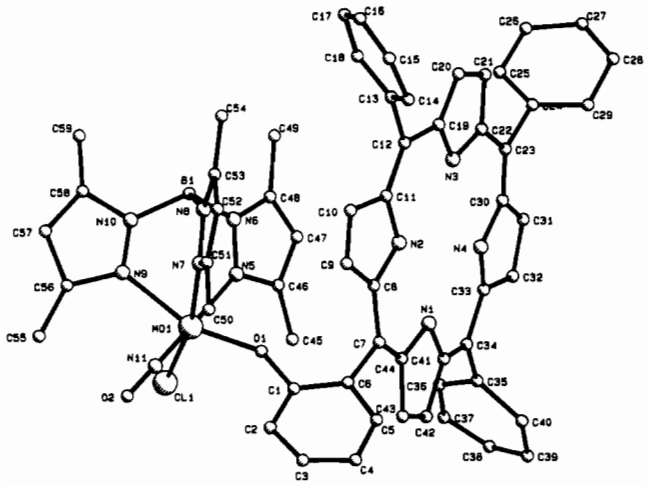

Figure 6. Molecular structure of **3**.

maximum deviations occurring at the α carbons of the pyrrole rings, C(8)/C(11), C(19)/C(22), C(30)/C(33), C(41)/C(44), alternately above and below the plane of the porphyrin inner ring, with the nitrogen atoms lying close to this plane. The porphyrin ring in **3**, however, ruffles in a less regular manner. Maximum deviations occur at the methine carbon atoms or α carbon atoms, C(7), C(11), C(22), and C(34), alternately above and below the plane of the porphyrin inner ring, and the nitrogen atoms are close to this plane.

In both structures, the porphyrin phenyl rings are planar to within experimental error and are twisted relative to the porphyrin plane in order to reduce steric interactions between the phenyl hydrogen atoms proximal to the porphyrin ring and the pyrrole hydrogen atoms.[39] The four phenyl rings in **1** and **3** are at angles of 110, 61, 55, 112 and 103, 59, 105, 82° (±2°), respectively, relative to the porphyrin plane.

From a consideration of the angles at molybdenum (Table 4), it can be seen that in both structures the molybdenum atoms show a slightly distorted octahedral coordination. Of the *trans* angles, the minimum angular deviation from the ideal octahedral angle of 180° occurs for the N−Mo−N(O) angle, whereas the other two angles deviate by larger amounts from ideality. This is in accord with the structures of other Mo(NO)Tp* moieties.[40−45]

The pyrazolyl rings in **1** and **3** are virtually planar. The methyl groups lie close to their respective ring planes, whereas the metal and boron atoms deviate by greater amounts, 0.22 and 0.14 Å (±0.05 Å) and 0.38 and 0.18 Å (±0.05 Å), respectively. The pyrazolyl ring planes are skewed relative to the molybdenum−boron axis in order to minimize steric interactions. As expected, the smallest dihedral angle is between the pyrazolyl rings encompassing the relatively small nitrosyl ligand. Within the rather large experimental error, there are no significant differences in the bond lengths and bond angles of the pyrazolyl rings.

In both **1** and **3**, the boron atom cannot interact with the metal for steric reasons (Mo···B = 3.3 Å and Mo···B = 3.2 Å, respectively). A study undertaken on 15 related complexes[40−45] has shown a mean distance of 3.23 Å for the Mo···B distance (minimum 3.2 Å;maximum 3.3 Å).

As usually found in this class of complexes, the molybdenum−nitrosyl fragment is nearly linear.[29] For the 15 complexes cited above, the mean value for the Mo−N−O angle is 176.6(5)° (minimum 173.2°; maximum 179.6°). Such a near-linear Mo−N−O arrangement allows the nitrosyl group to act as a three-electron donor, donating a lone pair of electrons of the nitrogen atom and a single π^* electron. The mean Mo−N bond length is 1.760(6) Å (minimum 1.698 Å; maximum 1.804 Å) and mean N−O bond length is 1.184(9) Å (minimum 1.097 Å; maximum 1.242 Å). In **1**, the values fall within these ranges (Table 4). However, in **3**, the short Mo−N and long N−O bond distances fall outside these ranges (Table 4) but, bearing in mind the large esd's, not significantly so. The sum of the two distances is, however, similar to the previous determinations (Table 4).

(39) Meyer, E. F., Jr.; Cullen, D. L. In *The Porphyrins*; Dolphin, D, Ed.; Academic Press: New York, 1978; Vol. 3, Chapter 11, pp 513−529.
(40) McCleverty, J. A.; Seddon, D.; Bailey, N. A.; Walker, N. W. *J. Chem. Soc., Dalton Trans.*, **1976**, 898−908.
(41) McCleverty, J. A.; Drane, A. S.; Bailey, N. A.; Smith, J. M. A. *J. Chem. Soc., Dalton Trans.* **1983**, 91−96.
(42) Jones, C. J.; McCleverty, J. A.; Neaves, B. D.; Reynolds, S. J.; Adams, H.; Bailey, N. A.; Denti, G. *J. Chem. Soc., Dalton Trans.* **1986**, 733−741.
(43) McCleverty, J. A.; Rae, A. E.; Wolochowicz, I.; Bailey, N. A.; Smith, J. M. A. *J. Chem. Soc., Dalton Trans.* **1982**, 429−438. McCleverty, J. A.; Denti, G.; Reynolds, S. J.; Drane, A. S.; El-Murr, N.; Rae, A. E.; Bailey, N. A.; Adams, H.; Smith, J. M. A. *Ibid.* **1983**, 81−89. McCleverty, J. A.; Rae, A. E.; Wolochowicz, I.; Bailey N. A.; Smith, J. M. A. *Ibid.* **1983**, 71−80. Adams, H.; Bailey, N. A.; Denti, G.; McCleverty, J. A.; Smith, J. M. A.; Wlodarczyk, A. *Ibid.* **1983**, 2287−2292. Das, A.; Jeffery, J. C.; Maher, J. P.; McCleverty, J. A.; Schatz, E.; Ward, M. D.; Wollermann, G. *Inorg. Chem.* **1993**, *32*, 2145−2155.
(44) Al Obaidi, N.; Hamor, T. A.; Jones, C. J.; McCleverty, J. A.; Paxton, K. *J. Chem.Soc., Dalton Trans.* **1986**, 1525−1530. McCleverty, J. A.; Rae, A. E.; Wolochowicz, I.; Bailey, N. A.; Smith, J. M. A. *Ibid.*, **1982**, 951−965. Denti, G.; Ghedini, M.; McCleverty, J. A.; Adams, H.; Bailey, N. A. *Transition Met. Chem.* **1982**, *7*, 222−224. Al Obaidi, N.; Brown, K. P.; Edwards, A. J.; Hollins, S. A.; Jones, C. J.; McCleverty, J. A.; Neaves, B. D. *J. Chem. Soc., Chem. Commun.* **1984**, 690−692. Al Obaidi, N.; Hamor, T. A.; Jones, C. J.; McCleverty, J. A.; Paxton, K. *J. Chem. Soc., Dalton Trans.* **1987**, 1063−1069.
(45) Al Obaidi, N.; Hamor, T. A.; Jones, C. J.; McCleverty, J. A.; Paxton, K. *J. Chem. Soc., Dalton Trans.* **1987**, 2653−2660.

In **1** and **3**, the Mo−Cl bond lengths of 2.366(3) and 2.382(9) Å, respectively, are shorter than the published data for Mo^{II}−Cl distances (2.42−2.56 Å)[46] but are comparable to the Mo−Cl bond lengths in related $\{Mo(NO)Tp^*\}^{2+}$ complexes.[40,45] The Mo−Cl bond lengths are slightly shorter than expected for a pure σ-bond, and consequently some small degree of π-donation from the halogen to the metal seems probable.[40]

In both **1** and **3**, the Mo−N(nitrosyl) bond is the shortest of all the Mo−N bonds (Table 4). The Mo−N *trans* to the strongly π-accepting nitrosyl group tends to be the longest of all the Mo−N(pyrazolyl) bonds as a result of the *trans* π-bonding effect. The Mo−N bond *trans* to the halogen is the shortest of all the Mo−N(pyrazolyl) bonds. This is a result of the smaller degree of π-bonding between the molybdenum and the halogen than between the molybdenum and the other two monodentate ligands. These findings are consistent with previous work.[40−45]

In both **1** and **3**, the $Mo-OC_6H_4porphH_2$ bond lengths are relatively short (Table 4). This implies significant pπ−dπ donation from the donor atom (O) to the coordinatively-unsaturated metal. The large Mo−O−C(1) angle is also consistent with pπ−dπ donation from the ligand to the metal, although steric effects may also play a role in increasing this angle to relieve any close contact between atoms. A study carried out on four oxido complexes[40,42,44] has shown a range of 129−134° for the Mo−O−C(1) angles with a mean value of 131.7(7)°. A comparison of the Mo−O−C(1) angles for **1** [132.7(7)°] and **3** [146.3(22)°] shows that the Mo−O−C(1) angle is greater in the *ortho* compound, presumably as a result of greater steric strain. In both **1** and **3**, the N(11)−Mo−O−C(1) torsion angles are small and are similar to values found previously.[40,42,44] Similar structural features are found also in the crystal structure of $[\{o\text{-}[Mo(NO)Tp^*Cl]NHC_6H_4\}Ph_3porphH_2]$.[47]

As noted earlier, the ^1H NMR spectrum of **3** contains a signal due to a pyrazolyl ring proton at a chemical shift of *ca.* 4 ppm upfield of its usual position. NOE studies on this compound suggested that one of the porphyrin pyrrole rings was interposed between two of the Tp* pyrazolyl rings. Because of these observations, and despite the fact that the NMR studies were performed in the solution phase, the solid state structure of **3** was examined to see if any unusual interactions existed which could explain these phenomena. The N(2)−C(8)−C(9)−C(10)−C(11) porphyrin pyrrole ring appears to be in close proximity to the N(7)−N(8)−C(53)−C(52)−C(51) pyrazolyl ring. The interatomic distances H(9)···C(51), H(10)···C(52), and H(10)···C(53) are all *ca.* 2.9 Å, whereas H(9)/H(10) distances to the N(5)−N(6)−C(48)−C(47)−C(46) pyrazolyl ring are all in excess of 4.4 Å. From the solid state structure, it appears that it is the H(10)···C(53) interatomic distance of *ca.* 2.9 Å which is responsible for the signal which is shifted upfield. The NOE studies are explained by the close proximity of the porphyrin pyrrole ring to both the N(7)−N(8)−C(53)−C(52)−C(51) and N(5)−N(6)−C(48)−C(47)−C(46) pyrazolyl rings, although in the solid state the porphyrin pyrrole ring appears to be closer to the former. The NOE findings suggest that in the solution phase the porphyrin pyrrole ring moves between both of the adjacent Tp* pyrazolyl rings. The solid state structure of $[\{o\text{-}[Mo(NO)Tp^*Cl]NHC_6H_4\}Ph_3porphH_2]$[47] was also examined for any analogous interactions, but none were found. This finding is consistent with the spectral properties of the anilido complex.

Conclusions. The peripherally-molybdenated tetraphenylporphyrin complexes exhibit rich electrochemical behavior. Thus most complexes exhibit two anodic and two cathodic processes associated with oxidation and reduction of the porphyrin ring while the molybdenum fragment undergoes a further well-resolved one-electron reduction. However, the potentials of the two redox fragments appear to be minimally influenced by the other's presence, probably because of poor transmission of Coulombic effects through the phenol ring which is partially rotated out of the plane of the porphyrin ring. Thus there is no "communication" between the inorganic and organic redox fragments in the solution (the "ground state"), on the basis of the electrochemical behavior of these complexes and in addition their electronic absorption and infrared spectroscopic characteristics. This contrasts with the photochemical behavior of these molecules, where we have shown[14] that the observed fluorescence quenching is due to fast intramolecular charge separation which produces transient species with lifetimes in the range 120−220 ps (communication via an "excited state"). We have therefore shown that photochemically-induced electron transfer from a porphyrin moiety to an adjacent metal acceptor is a viable and rapid process, which can occur reversibly. Furthermore, the $\{M(NO)Tp^*(X)(E-)\}$ (M = Mo, W; X = halide, alkoxide; E = O, S, NH) moiety provides a highly versatile redox center, the reduction potential of which may be varied over a range exceeding 1 V.[29] Thus this class of compounds offers an important opportunity to investigate how the rate of electron transfer from the photoexcited porphyrin to the peripheral metal center varies with $\Delta G°$ for the charge separation process. The findings reported here demonstrate that such a study is feasible and represent the first stage of such a study.

Acknowledgment. We are grateful to the SERC (N.M.R., S.S.K., N.N.P.), the Erasmus programme (J.-D.F), and the Wolfson (Scotland) Trust (E.J.L.M.) for support of this work, the Politechnika Krakowska for leave of absence (S.S.K.), Drs. R. J. Goodfellow and M. Murray of the University of Bristol for assistance with NOE work, and Mr. T. Green for technical assistance.

Supporting Information Available: Full listings of H atom coordinates, bond distances and angles, and anisotropic thermal parameters (14 pages). Ordering information is given on any current masthead page.

IC950068T

(46) Chaiwasie, S.; Fenn, R. H. *Acta Crystallogr*, **1968**, *B24*, 525−529. Mawby, A.; Pringle, G. E. *J. Inorg. Nucl.Chem.* **1972**, *34*, 517−524. Kirchner, R. M.; Ibers, J. A.; Saran, M. S.; King, R. B. *J. Am. Chem. Soc.* **1973**, *95*, 5775−5776. Visscher, M. O.; Caulton, K. G. *J. Am. Chem. Soc.* **1972**, *94*, 5923−5924.

(47) Rowley, N. M.; Kurek, S. S.; Hamor, T. A.; Jones, C. J.; McCleverty, J. A. Work to be published.

(48) Molybdenum has two spin-active isotopes with spin 5/2, hence it was expected to observe a six line signal due to these isotopes, with a large unsplit central signal due to the remaining molybdenum isotopes with no nuclear spin. The two molybdenum spin-active isotopes, $^{95}_{42}Mo$ and $^{97}_{42}Mo$ (natural abundances 15.72% and 9.46%), have very similar nuclear magnetic moments of −0.013 and −0.933 μN. The hyperfine coupling constants are therefore sufficiently similar that two sets of signals cannot be distinguished, and the spectra can be adequately explained by considering the 25.2% of the signal intensity is split into a 1:1:1:1:1:1 sextet with the other 74.8% as a central single peak.